

## CHAPTER 6

---

# OPERATIONS

---

### 6.1 OPERATIONS EXECUTIVE SUMMARY

The purpose of this chapter is to address different ways that a low-energy transfer may impact the operations of a spacecraft, compared to conventional lunar transfers. Most conclusions are very straightforward consequences of the fact that low-energy transfers require less change in velocity ( $\Delta V$ ), more time, and have longer link distances during the transfer than direct lunar transfers. For instance, there are fewer demands on the spacecraft's propulsion system and operational schedule, but more demands on the spacecraft's communication capabilities due to the longer distances. The operations team must be able to perform several trajectory correction maneuvers (TCMs) during the trans-lunar cruise, but these maneuvers are typically much more separated in time from launch, lunar arrival, and other maneuvers than they are on conventional lunar transfers.

The majority of discussion in this chapter is devoted to studying the availability and  $\Delta V$  cost of establishing an extended 21-day launch period for a lunar mission. Conventional lunar missions typically have very constrained launch periods, reflecting the geometry in the Sun–Earth–Moon system. However, low-energy lunar

transfers are very flexible and may be adjusted in many ways to accommodate an extended launch period. Several conclusions are drawn from these examinations.

First, the cost of a launch period is dependent on the number of launch days in the period. The examination performed in Section 6.5 estimates that it costs on average 2.5 meters per second (m/s) of  $\Delta V$  per day added to a launch period; hence, the average 21-day launch period requires about 50 m/s more deterministic  $\Delta V$  than a 1-day launch period for a given transfer. The cost of the 1-day launch period is dependent on the inclination change that must be performed to inject onto the desirable low-energy transfer from a constrained low Earth orbit (LEO) parking orbit. Section 6.5.7 estimates that it costs approximately 0.97 m/s more transfer  $\Delta V$  per degree of inclination change that must be performed. The total cost of establishing a 21-day launch period from a 28.5-degree (deg) LEO parking orbit to a given lunar orbit is approximately  $71.7 \pm 29.7$  m/s ( $1\sigma$ ). Thus, to be very conservative when estimating a preliminary  $\Delta V$  budget for a mission, one may estimate that the  $\Delta V$  cost to transfer from a 28.5-deg LEO parking orbit to a particular lunar orbit, including a 21-day launch period, will cost approximately 161 m/s, not including statistical costs and/or other deterministic costs. Of course, the 161 m/s accounts for a 3-sigma high value, evaluated from a large set of random mission designs; it is likely that a practical mission may be constructed for significantly less  $\Delta V$ .

A 21-day launch period does not necessarily have to include 21 consecutive days; in fact, most launch periods constructed in this examination include one or two gaps when the launch operations would have to stand down. The average launch period for the sample set used here requires a total of 27 days; the vast majority of the launch periods may be contained within 40 days.

Finally, it has been found that there is no significant trend between the total launch period  $\Delta V$  for the sample missions studied here and their reference departure inclination values or their reference transfer durations, except that missions with short durations ( $< 90$  days) require more  $\Delta V$  to establish an extended launch period, on account of the reduced flexibility of a shorter transfer.

## 6.2 OPERATIONS INTRODUCTION

This chapter discusses several aspects of a spacecraft mission that must be considered for the low-energy transfers presented in this book to be used in a real mission. Numerous discussions throughout Chapters 3–5 have considered the latitude of the mission's launch site, since that strongly influences the inclination of the parking orbit that may be used in a mission. But other aspects have not been fully discussed, such as which launch vehicle may be used, how to establish a launch period, and what considerations must be made to a spacecraft's design to fly a low-energy transfer.

Sections 6.3 and 6.4 provide information and discussion about which launch sites and launch vehicles are typically used and/or available for lunar missions. Section 6.5 provides a lengthy discussion, analysis, and several algorithms that may be used to generate a 21-day launch period for a given low-energy transfer. The results indicate that simple low-energy transfers may be targeted from nearly any LEO parking

orbit with a 21-day launch period for a modest fuel cost on the order of 72 m/s. Section 6.6 discusses issues relevant to navigating a spacecraft while on a low-energy transfer, including the costs of station-keeping and the benefits of having 3–4 months to perform the transfer instead of the conventional 3–6 days. Finally, Section 6.7 presents several considerations that must be made to the spacecraft systems and operations design to accommodate a low-energy lunar transfer.

### 6.3 LAUNCH SITES

Chapters 3–5 illustrated that low-energy ballistic transfers may be constructed that depart the Earth from parking orbits or direct departures with any orbital inclination. By carefully selecting a particular transfer, one may build a mission that launches from any given launch site and efficiently injects into the ballistic lunar transfer. While this is very important for conventional mission design, Section 6.5 later demonstrates that a mission can actually depart the Earth from virtually any inclination and transfer to a particular lunar arrival for a modest  $\Delta V$  cost. Still, it is of interest to build a low-energy transfer that is designed to depart the Earth with an inclination that is very similar to the latitude of the mission's launch site so that no sizable orbital plane changes are needed. This is particularly useful for missions with a brief launch period.

Table 6-1 provides a summary of the launch sites that have demonstrated the capability of placing large payloads into orbit. This is not a complete list, but provides a good review of the latitude and longitude of several sites for reference.

### 6.4 LAUNCH VEHICLES

Many launch vehicles are available to place spacecraft on low-energy lunar transfers. The NASA Launch Services Program (LSP) at Kennedy Space Center coordinates contracts with several launch vehicle providers using NASA Launch Services (NLS) contracts [211]. On September 16, 2010, NASA released the details about the NLS II contracts that were awarded to four launch vehicle providers: Lockheed Martin Space Systems Company of Denver, Colorado; Orbital Sciences Corporation of Dulles, Virginia; Space Exploration Technologies of Hawthorne, California; and United Launch Services, LLC of Littleton, Colorado. This contract includes several families of launch vehicles, including Atlas V, Falcon 9, Pegasus XL, Taurus XL, Athena I, and Athena II. The NLS II contract provides the minimum performance that is contractually obligated by the launch vehicle; a mission may be able to negotiate with the launch vehicle provider to increase the performance of the launch vehicle depending on the mission's requirements [211].

Table 6-2 summarizes the maximum payload capabilities of several launch vehicles injected from Cape Canaveral, Florida, onto low-energy lunar transfers with and without an outbound lunar flyby. The table captures two extreme cases: first, the case where the transfer includes an outbound lunar flyby and requires an injection  $C_3$  of  $-2.1$  kilometers squared over seconds squared ( $\text{km}^2/\text{s}^2$ ), which is near the

**Table 6-1** The locations of several launch sites that have been used to launch large payloads into orbit, toward the Moon, and/or into Interplanetary space. This is not a complete list, the locations are approximate, and some are representative of several particular launch sites.

Country	Location	Latitude (deg)	Longitude (deg)	Comments
USA	Cape Canaveral Air Force Station, Florida	28.47 N	80.56 W	Interplanetary
USA	Kennedy Space Center, Florida	28.61 N	80.60 W	Lunar
USA	Vandenberg Air Force Base, California	34.77 N	120.60 W	High inclinations
USA	Kodiak Launch Complex, Alaska	57.44 N	152.34 W	Orbital
USA	Mid-Atlantic Regional Spaceport (MARS), Delmarva Peninsula, Virginia	37.83 N	75.48 W	Orbital
USA	Kwajalein Atoll	9.00 N	167.65 E	Orbital
Brazil	Alcântara Launch Center, Maranhão	2.32 S	44.37 W	Orbital
China	Jiuquan Satellite Launch Center	41.12 N	100.46 E	Orbital
China	Xichang Satellite Launch Center	28.25 N	102.03 E	Lunar
French Guiana	Guiana Space Centre, Kourou	5.24 N	52.77 W	Interplanetary
India	Satish Dhawan Space Centre (Sriharikota), Andhra Pradesh	13.74 N	80.24 E	Lunar
Israel	Palmachim Air Force Base	31.88 N	34.68 E	Orbital
Japan	Uchinoura Space Center	31.25 N	131.08 E	Orbital
Japan	Tanegashima Space Center, Tanegashima Island	30.39 N	130.97 E	Orbital
Kazakhstan	Baikonur Cosmodrome, Tyuratam	45.96 N	63.35 E	Interplanetary
Marshall Island	Omelek	9.05 N	167.74 E	Orbital
Russia	Svobodny Cosmodrome, Amur Oblast	51.83 N	128.28 E	Orbital
Russia	Yasny Cosmodrome, Orenburn Oblast	51.21 N	59.85 E	Orbital
Russia	Kapustin Yar Cosmodrome, Astrakhan Oblast	48.58 N	46.25 E	Orbital
Sweden	Esrange, Kiruna	67.89 N	21.10 E	Orbital
Several	Sea Launch / Ocean Odyssey complex	0.0 N	Varies	Orbital

**Table 6-2** The payload capabilities of several launch vehicles injected from Cape Canaveral, Florida, onto low-energy lunar transfers with and without an outbound lunar flyby. This information has been captured from the NASA Launch Services (NLS) Program's Launch Vehicle Performance site under the NLS II contract [211].

Launch Vehicle	Maximum Payload Performance (kg)	
	$C_3 = -2.1 \text{ km}^2/\text{s}^2$	$C_3 = -0.3 \text{ km}^2/\text{s}^2$
Athena II	395.0	375.0
Falcon 9 Block 1	2125.0	1995.0
Falcon 9 Block 2	2645.0	2515.0
Atlas V 401	3170.0	3050.0
Atlas V 411	4095.0	3955.0
Atlas V 421	4845.0	4680.0
Atlas V 431	5445.0	5265.0
Atlas V 501	2215.0	2110.0
Atlas V 511	3410.0	3285.0
Atlas V 521	4365.0	4215.0
Atlas V 531	5135.0	4965.0
Atlas V 541	5815.0	5625.0
Atlas V 551	6340.0	6140.0

minimum injection energy typically required. The second case presented requires a  $C_3$  of  $-0.3 \text{ km}^2/\text{s}^2$ , which is near the maximum injection energy typically required without a lunar flyby. Most missions will fall between these two values: closer to one depending on whether or not the mission aims to fly past the Moon on the outbound segment.

As of September 2011, Orbital Sciences estimates that the Taurus XL may be used to inject as much as 425 kilograms (kg) to a  $C_3$  of  $0 \text{ km}^2/\text{s}^2$ , and presumably more to a low-energy lunar transfer. Further, although it is not currently in the NLS II contract, Orbital Sciences estimates that the Taurus II launch vehicle may be able to inject between 920 kg and 1120 kg to a  $C_3$  of  $-2.1 \text{ km}^2/\text{s}^2$  depending on its configuration. The Taurus II's performance drops about 40 kg when injecting payloads to a  $C_3$  of  $-0.3 \text{ km}^2/\text{s}^2$ .

In addition, the Pegasus XL launch vehicle may be used to place up to about 470 kg of payload into a 200-km circular parking orbit [212]. A spacecraft could then perform its own trans-lunar injection to transfer to the Moon, much like the proposed *Dust Near Earth (DUNE)* mission [146, 213], or similar to the *Interstellar Boundary Explorer (IBEX)* mission [214–216].

Other launch vehicles may also be used to inject a spacecraft onto a low-energy lunar transfer, though they do not have a contract with NASA, including the Delta IV family of vehicles. Certainly several international vehicles may be used, assuming the

vehicles' guidance algorithms have the capability of targeting such orbital parameters, including the Russian Soyuz and Proton vehicles, Arianespace's Ariane V, China's Long March and CZ vehicles, Japan's H-IIA and H-IIB, and Ukraine's Zenit-3SL, among others. The Indian Space Research Organization's (ISRO's) Polar Satellite Launch Vehicle (PSLV-C11) was used to launch the *Chandrayaan-1* mission to the Moon, though the launch vehicle only injected the spacecraft into a 6-hour orbit about the Earth and the spacecraft performed the remainder of the lunar injection.

## 6.5 DESIGNING A LAUNCH PERIOD

This section considers how to construct an extended launch period for a low-energy transfer to the Moon. The discussion begins by reviewing several interesting features that exist in the Earth–Moon system and how historical launch periods have been constructed around those features. This provides context for future discussions about designing launch periods for low-energy transfers.

First, the Moon's orbit is nearly circular about the Earth. This means that one may theoretically launch a spacecraft on a conventional, direct transfer with very similar characteristics on any given day. The Moon's elliptical orbit means that the launch energy and transfer duration will vary across the month to some degree, but this is a second-order effect. The largest variation from one day to the next when injecting into a direct transfer arises from the obliquity of the Earth relative to the Moon's orbit. The Earth's spin axis is tilted approximately 23.5 deg relative to the ecliptic, and the Moon's orbit has an inclination of about 5.15 deg with respect to the ecliptic. Together, this means that the relative orientation of the Earth's spin axis and the orbit of the Moon may be anywhere from 18.35 deg to 28.65 deg; the orientation of the parking orbit must be adjusted to accommodate this shift. Ultimately this means that the time of day that one must launch shifts from one day to the next, as does the duration of time that the spacecraft coasts in a low Earth parking orbit prior to injecting toward the Moon.

Next, a lunar day is approximately 29.5 Earth days long, which means that the lighting conditions on the Moon roughly repeat every 29.5 days. There are variations on top of this cycle that correspond with where the Moon is in its orbit about the Earth relative to its perigee, and where the Earth is in its orbit about the Sun. The net effect is that if one is interested in viewing a particular lighting condition as one flies by the Moon or impacts the Moon, then one may only be able to launch on a direct transfer one or two days every month. This is very important for missions that aim to land on the surface, including the Apollo missions. The Apollo missions were designed to land on the surface soon after sunrise at the landing site to maximize the amount of sunlit time they had on the surface before needing to ascend. These considerations have a direct effect on the time of arrival at the Moon for any mission, though missions that go into orbit prior to landing/impact can arrive early. The time of arrival is highly correlated with the launch time for direct transfers, since direct transfers have a short transfer duration that cannot be varied much. The time of arrival is loosely correlated with the launch time for low-energy transfers, since low-energy

transfers can vary their transfer durations by many days without a large penalty in transfer  $\Delta V$ .

Another consideration for a mission planner is that many lunar spacecraft are not designed to survive a long eclipse. Lunar eclipses occur roughly every 6 months when the Earth comes directly between the Sun and Moon. The Moon's nonzero orbital inclination relative to the ecliptic means that a lunar eclipse does not occur each and every month, but only occurs when the Moon is near its ascending or descending node when it traverses behind the Earth. Since the Moon's orbit is fixed in inertial space, though subject to perturbations, one of the nodes traverses directly behind the Earth twice per year. If the Moon is near that point in its orbit at that time, then the eclipse will be a full lunar eclipse and any spacecraft on the surface or in a low orbit will traverse through the umbra of the Earth. If the Moon is not near that point in its orbit, then the spacecraft may be able to avoid the shadow, or at least avoid the umbra of the Earth. The *Gravity Recovery and Interior Laboratory (GRAIL)* mission was designed with lunar eclipses in mind, since the two *GRAIL* spacecraft were not originally designed to survive an extended passage through shadow. *GRAIL*'s entire science phase was designed to occur between two lunar eclipses in case one of the spacecraft did not survive the following eclipse. This means that *GRAIL*'s launch opportunities do not repeat every month, but only repeat once every six months.

### 6.5.1 Low-Energy Launch Periods

Low-energy lunar transfers are more flexible than direct lunar transfers since their transfer durations are longer; hence, it is possible to build an extended, 21-day launch period such that every launch opportunity yields a trajectory that a spacecraft can follow that arrives at the Moon at the same time. This is very useful for missions such as *GRAIL* that depend on arriving at the Moon at a particular time of the year or month.

There are often many ways to adjust a trajectory's design so that it may depart the Earth on multiple days, in order to establish a launch period. For this discussion we assume that the trajectory begins with a launch from a particular site into a low, near-circular parking orbit; coasts in the parking orbit for some duration; performs a trans-lunar injection; and then follows a ballistic transfer to the Moon using one or two trajectory correction maneuvers en route to the Moon. Given this trajectory design, several examples of controls include the following:

- Adjust the launch time. By launching at a different time of day, one can change the longitude of the ascending node of the parking orbit that the spacecraft uses prior to its trans-lunar injection.
- Adjust the launch and parking orbit geometry. One may be able to reduce the total transfer  $\Delta V$  cost and ultimately transfer more payload mass to the Moon by changing the parking orbit's inclination. This reduces the launch vehicle's performance, but it may be worthwhile.
- Adjust the location of the trans-lunar injection maneuver in the parking orbit.

- Adjust the trans-lunar injection maneuver. The maneuver magnitude and/or direction may be adjusted, depending on the control algorithm that operates the maneuver. In the studies presented in this chapter, only the maneuver magnitude is adjusted.
- Add one or more trajectory correction maneuvers in the trans-lunar cruise. These maneuvers may be performed in any direction, though some missions may place constraints on the magnitude or direction of these maneuvers. In the studies presented here, two maneuvers are introduced that may be performed in any direction with any maneuver magnitude, though no two maneuvers may be placed within four days of each other to reduce operations complexity.
- Adjust the lunar arrival conditions as described below.

The available controls upon arriving at the Moon depend on the arrival orbit/geometry and the mission design. Some examples of different missions and their controls include:

**Arriving at a lunar libration orbit.** Arriving at a lunar libration orbit typically involves a ballistic, asymptotic arrival with a final correction maneuver to ensure that the spacecraft is placed in the target orbit. Controls include:

- Adjust the date/time of arrival. This may vary by mere seconds or by days, depending on the mission's requirements.
- Vary the target libration orbit. It is typically more desirable to maintain a single target libration orbit throughout the launch period, though that depends on the mission.
- Add a libration orbit insertion maneuver, which may vary in magnitude/direction. This is typically much more useful if the target libration orbit is held fixed across a launch period.

**Arriving at a low lunar orbit.** Arriving at a low lunar orbit typically involves a time-critical lunar-orbit insertion (LOI) maneuver that places the spacecraft into a capture orbit. Controls include:

- Adjust the date/time of the LOI. This may vary by mere seconds or by days, depending on the mission's requirements.
- Adjust the LOI's magnitude and/or direction. Some spacecraft designs require that the maneuver be a fixed-attitude maneuver, a pitch-over maneuver, or a maneuver that rotates about a specified axis at a constant rate. The studies presented here model the maneuver using an impulsive burn and frequently permit the burn to vary in both magnitude and direction.
- Adjust the location of the LOI within the target orbit. This is typically held constant, or varied only a small amount, since the maneuver is much more efficient when performed at the orbit's periapse.



- Adjust the geometry of the capture orbit. The spacecraft's mission design may permit the orbit's argument of periapse to vary, particularly if the goal is to eventually enter a circular orbit. It may also be permissible to vary the inclination or longitude of ascending node of the orbit, though those are typically not varied more than a small amount.

**Arriving at the lunar surface.** A mission to the lunar surface may be targeting a shallow flight path angle with the goal to land softly, or it may be targeting a steep flight path angle for a targeted impact, similar to the design of the *Lunar Crater Observatory and Sensing Satellite (LCROSS)* mission. Some examples of trajectory controls include:

- Adjust the date/time of arrival. This may vary by mere seconds or by days, depending on the mission's requirements.
- Adjust the arrival velocity.
- Adjust the arrival geometry. It may be permissible to vary the flight path angle and/or azimuth of the arrival.
- Adjust the arrival location on the lunar surface.

In addition, it may be possible to incorporate a dramatic shift in a mission's trajectory. For instance, it may be preferable to break a 21-day launch period into two halves, where the early portion of the launch period sends the spacecraft toward the Sun–Earth  $L_1$  vicinity and the second portion implements trajectories that travel near the Sun–Earth  $L_2$  vicinity.

One can see that there are many ways to adjust a trajectory from one launch opportunity to the next in order to establish a launch period. This section presents several scenarios and their corresponding algorithms that may be used to establish a launch period. The algorithms presented here may need to be adjusted for a particular mission, though the results presented here are certainly useful for guiding the early trades for a mission.

### 6.5.2 An Example Mission Scenario

There are many ways to construct an extended launch period for a low-energy lunar transfer, some of which are outlined above. This section studies one mission design architecture and applies that to a large number of practical cases, in order to generate some useful statistics about that architecture. The design studied here is similar to *GRAIL*'s mission: a spacecraft is launched from a parking orbit that has an inclination of 28.5 deg, for example, one that effectively supports launches from Cape Canaveral, and uses a near-ballistic low-energy transfer to target a low, 100-km, polar orbit about the Moon. The trajectory includes as many as two deterministic trajectory correction maneuvers (TCMs) to assist the construction of a 21-day launch period. The results of the studies presented here for this architecture are (of course) only relevant to

very similar missions, but hopefully they shed some light on other low-energy lunar architectures.

Figure 6-1 illustrates one example trajectory taken from the surveys presented in Section 4.4. This trajectory departs the Earth on April 1, 2010, at 05:27 Coordinated Universal Time (UTC) from a 185-km parking orbit with an inclination of approximately 38.3 deg and transfers to the Moon using no maneuvers at all. It arrives at a polar orbit 100 km above the mean radius of the Moon. A launch vehicle may certainly target an outbound inclination of 38.3 deg on that date to inject a spacecraft onto this transfer, but it would suffer a large penalty to its lift capability if it did so from Cape Canaveral, compared to the vehicle's capability to lift payloads to an inclination of 28.5 deg. Further, the launch may slip. This section studies how to adjust the transfer to permit it to depart the Earth from an inclination of 28.5 deg on multiple days. As an example, a new trajectory has been generated using the ballistic transfer shown in Fig. 6-1 as a reference. The new trajectory departs the Earth a full day after the reference, on April 2, 2010, and departs from a 28.5 deg parking orbit. Two maneuvers are required to correct this new outbound trajectory so that it arrives at the same lunar orbit as the reference. Figure 6-2 illustrates the difference between

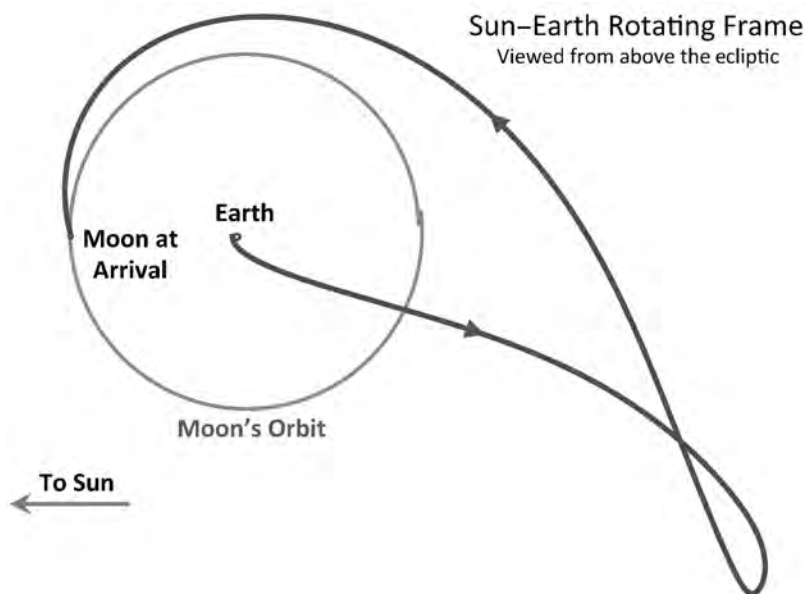


**Figure 6-1** An illustration of the example reference low-energy lunar transfer, shown in the Sun-Earth rotating frame from above the ecliptic, where the Sun is fixed to the left [190] (Copyright © 2012 by American Astronautical Society Publications Office, San Diego, California (Web Site: <http://www.univelt.com>), all rights reserved; reprinted with permission of the AAS).

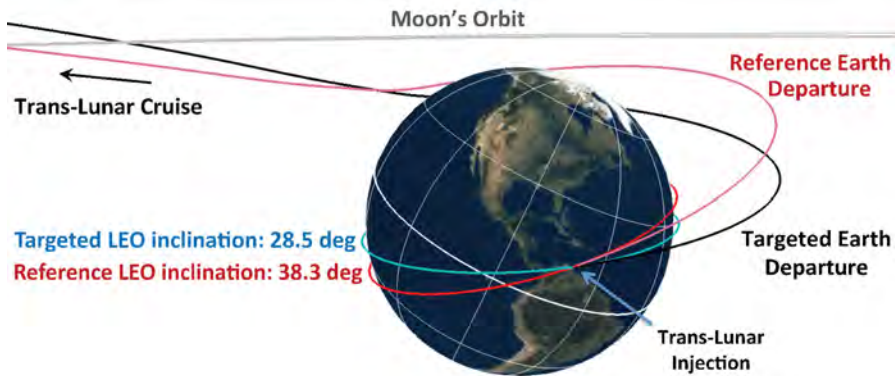


**Figure 6-2** The targeted Earth departure compared with the reference Earth departure [191] (*Acta Astronautica* by International Academy of Astronautics, reproduced with permission of Pergamon in the format reuse in a book/textbook via Copyright Clearance Center). (See insert for color representation of this figure.)

the Earth departures of the reference trajectory and the newly adjusted trajectory. Figure 6-3 shows the difference between these transfers, as viewed from above in the Sun–Earth rotating reference frame. Finally, Fig. 6-4 shows a top-level view of 21 such trajectories that depart the Earth on 21 different days and all arrive at the Moon at the same time at the same orbit. The details of these trajectories, and whether or not they should vary in any given way, is described later.

The performance of the launch period for this example mission depends on which controls are available. For instance, if one is only permitted to vary the launch time and the trans-lunar injection, while keeping the dates of the trajectory correction maneuvers constant and keeping the geometry of the lunar orbit insertion constant, then the spacecraft must be capable of performing at least 730 m/s of  $\Delta V$  to reach a 100-km circular polar orbit about the Moon. But if the dates of the TCMs are permitted to vary as well as the magnitude and direction of the lunar orbit insertion, then the spacecraft's fuel budget may be reduced such that it must perform only 706 m/s of  $\Delta V$  on the most challenging launch day of a 21-day launch period. However, these controls may not be available to the mission. Figure 6-5 illustrates the total  $\Delta V$  that must be performed for a spacecraft in each of five different launch period configurations. One can see that the launch period  $\Delta V$  cost may be reduced even by adjusting a single parameter; for instance, Launch Period 3 requires approximately 10.7 m/s less  $\Delta V$  than Launch Period 2 and the only thing different is that the date of the second TCM is performed 10 days later in each trajectory.

The illustrations shown here are representative of one example lunar mission. This section explores several hundred such missions and characterizes any statistical

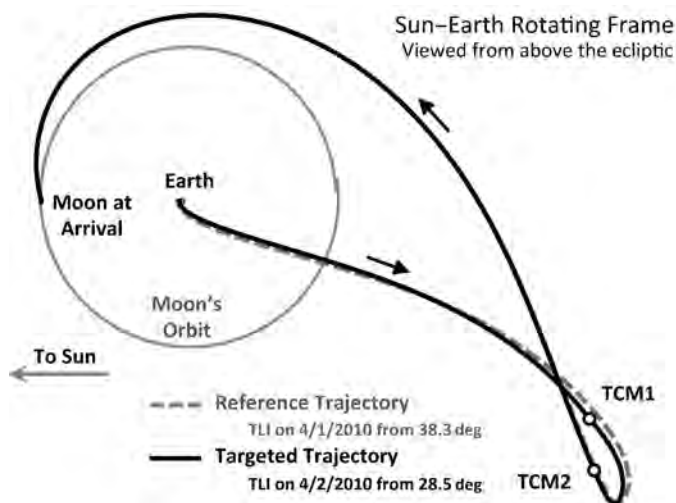


**Figure 6-3** The final targeted lunar transfer compared to the reference transfer, viewed in the Sun–Earth rotating frame from above the ecliptic [191] (*Acta Astronautica* by International Academy of Astronautics, reproduced with permission of Pergamon in the format reuse in a book/textbook via Copyright Clearance Center).

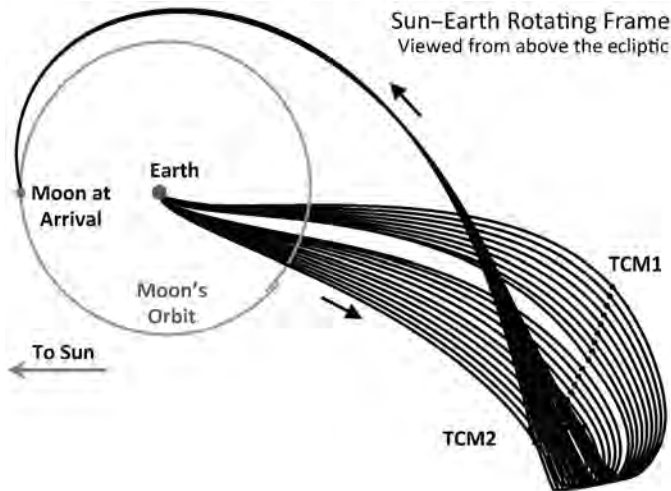


**Figure 6-4** An example of 21 trajectories that depart the Earth from 21 different days and all arrive at the Moon at the same time, inserting into the same lunar orbit. The trajectories are viewed in the Sun–Earth rotating frame from above the ecliptic.

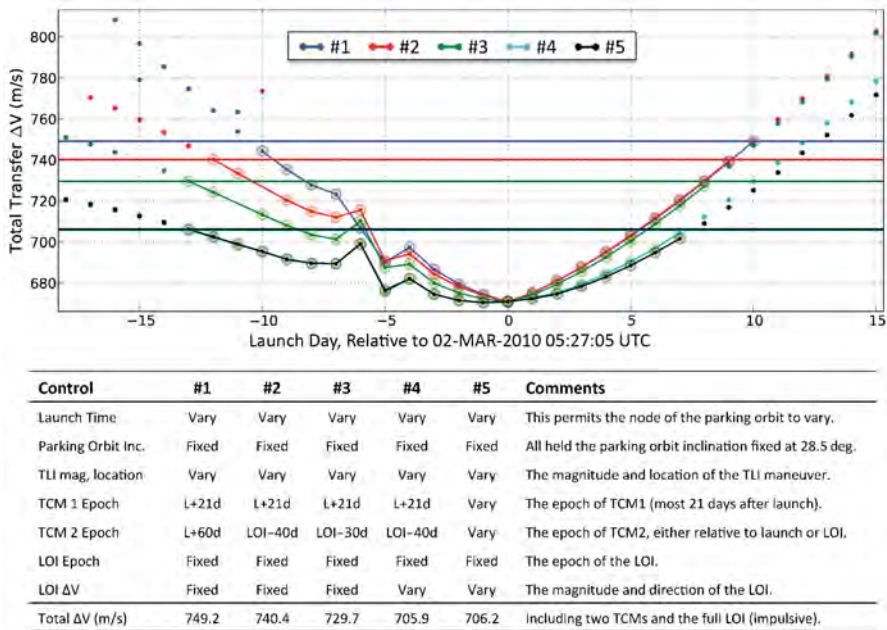


**Figure 6-5** Several example launch periods for the example lunar mission, depending on which controls are fixed, their fixed values, and which controls are permitted to vary. (See insert for color representation of this figure.)

findings that provide mission managers rules of thumb for estimating the costs of establishing a launch period for a given low-energy transfer.

### 6.5.3 Targeting Algorithm

Each lunar mission and its corresponding launch period is constructed here using a straightforward procedure that is described as follows. Once again, this algorithm is formulated for missions to low lunar orbits, though it may be easily modified for other destinations.

**Step 1.** First, a target lunar orbit is selected and a reference low-energy lunar transfer is constructed. The transfers used here have been taken from the surveys presented in Section 4.4, which provides many more details about these transfers, but to summarize, each transfer targets a low lunar orbit that is constructed by setting its semi-major axis to 1837.4 km, its eccentricity to zero, and its inclination to 90 deg in the International Astronomical Union (IAU) Moon Pole coordinate frame. This defines a circular, polar orbit with an altitude of approximately 100 km. Its longitude of ascending node,  $\Omega$ , and argument of

periapse,  $\omega$ , are selected from the surveys and can take on a wide variety of combinations.

An impulsive, tangential LOI is applied at the orbit's periapse point on a specified date. The LOI  $\Delta V$  magnitude is taken from the surveys. It is set to generate a trajectory that originates at the Earth via a simple low-energy transfer: one that contains no close lunar encounters or Earth-phasing orbits. The  $\Delta V$  value is at least 640 m/s and is the least  $\Delta V$  needed to construct a transfer that requires fewer than 160 days to reach an altitude of 1000 km or less above the Earth when propagated backward in time. Table 6-3 summarizes several example transfers that target low lunar orbits that each have an  $\Omega$  of 120 deg; these may be seen in the surveys illustrated in Figs. 4-6, 4-7, and 4-8 and in Table 4-4 in Section 4.4.

Each reference trajectory generated in this study has no maneuvers and does not target any particular Earth orbit when propagated backward in time.

**Step 2.** Second, the mission's LEO parking orbit and trans-lunar injection time are specified. The LEO parking orbits used in this study are all 185-km circular orbits with inclinations of 28.5 deg, as previously described. The orbit's node,  $\Omega_{\text{LEO}}$ , and the location of the trans-lunar injection (TLI) maneuver about the orbit,  $\nu_{\text{LEO}}$ , are permitted to vary; the TLI is performed impulsively and tangent to the orbit. The values of  $\Omega$  and  $\nu_{\text{LEO}}$  may initially be set to any arbitrary angle, for example, to 0 deg.

**Step 3.** If the LOI maneuver is permitted to vary, which it is in the majority of the missions studied here, then the third step is to adjust the low-energy transfer such that its perigee passage occurs at the time of the TLI. This is performed by searching for the smallest change in the LOI  $\Delta \vec{V}$  that results in a new low-energy transfer that originates at the Earth on the date of the TLI, or at

**Table 6-3** A summary of the performance parameters of several example simple low-energy lunar transfers. None of these transfers includes any Earth phasing orbits or lunar flybys [190] (Copyright © 2012 by American Astronautical Society Publications Office, San Diego, California (Web Site: <http://www.univelt.com>), all rights reserved; reprinted with permission of the AAS).

Traj #	$\Omega$ (deg)	$\omega$ (deg)	$\Delta V_{\text{LOI}}$ (m/s)	Duration (days)	LEO Inclination (deg)		$C_3$ (km <sup>2</sup> /s <sup>2</sup> )
					Equatorial	Ecliptic	
1	120.0	169.2	669.3	83.483	29.441	6.129	-0.723
2	120.0	103.8	692.1	85.287	25.688	34.778	-0.723
3	120.0	70.2	743.9	93.598	57.654	74.955	-0.667
4	120.0	225.3	716.0	93.621	134.322	112.840	-0.657
5	120.0	99.9	697.5	110.060	83.127	61.624	-0.697
6	120.0	186.9	673.2	122.715	23.941	3.088	-0.712

least one that has a perigee on that date even if the perigee altitude is higher than 1000 km. The optimization package sparse nonlinear optimizer (SNOPT) was used for the missions presented here, but other algorithms may certainly be used.

- Step 4.** The radius of the low-energy transfer with respect to the Earth at a time 20 days after the TLI is noted. The TLI  $\Delta V$  magnitude,  $\Delta V_{\text{TLI}}$ , is set to a value that takes the Earth-departure trajectory out to that distance at that time. The spacecraft is beyond the orbit of the Moon by that time, assuming no Earth-phasing orbits, and not yet at its apogee.
- Step 5.** The values of  $\Omega_{\text{LEO}}$  and  $\nu_{\text{LEO}}$  are adjusted to minimize the difference in position between the Earth-departure and the target low-energy transfer at a time 20 days after TLI. After convergence, the algorithm is repeated, this time permitting  $\Delta V_{\text{TLI}}$  to vary as well. It is typically the case that the Earth-departure trajectory will intersect the target low-energy transfer at that time when all three variables are permitted to vary, though it is not necessary. Once again this study implemented the SNOPT package to perform the optimization.
- Step 6.** Two deterministic maneuvers are added to the trajectory: TCM1 at a time 21 days after TLI, and TCM2 at a time halfway between TCM1 and LOI. It is intentional that the first maneuver be placed near 20 days but not at a value of 20 days in order to improve the performance of the optimization algorithm in the next step [183]. A single-shooting differential corrector (Section 2.6.5.1) may be used to target the values of  $\Delta V_{\text{TCM1}}$  and  $\Delta V_{\text{TCM2}}$  to generate a continuous end-to-end trajectory.
- Step 7.** Finally, all control parameters are varied using an optimizer to minimize the total transfer  $\Delta V$  of the trajectory. This study again used the SNOPT package to perform the optimization. The missions generated here permitted eight control variables to vary: the three Earth-departure parameters  $\Omega_{\text{LEO}}$ ,  $\nu_{\text{LEO}}$ , and  $\Delta V_{\text{TLI}}$ ; the dates of the two trans-lunar maneuvers  $t_{\text{TCM1}}$  and  $t_{\text{TCM2}}$ ; and the three components of the LOI  $\Delta V$ , namely,  $\Delta V_{\text{LOI}}^x$ ,  $\Delta V_{\text{LOI}}^y$ , and  $\Delta V_{\text{LOI}}^z$ . When the eight parameters are adjusted, an Earth-departure trajectory is generated out to the time of TCM1, a lunar-arrival trajectory is generated backward in time from LOI to the time of TCM2, and a bridge trajectory is generated connecting TCM1 and TCM2 using a single-shooting differential corrector (Section 2.6.5.1). The total transfer  $\Delta V$  that is minimized includes the sum of the maneuvers that are typically required by the spacecraft, namely, the sum of  $\Delta V_{\text{TCM1}}$ ,  $\Delta V_{\text{TCM2}}$ , and  $\Delta V_{\text{LOI}}$ , but not the TLI  $\Delta V$ . The dates of the TLI and LOI are fixed, and the dates of TCM1 and TCM2 are constrained to be at least four days from any other maneuver to facilitate relaxed spaceflight operations.

When the optimizer has converged, the performance of the trajectory compared with the reference low-energy transfer is recorded. It is often the case that the differential corrector will converge on a local minimum and not the global minimum;

hence, this process is repeated with adjustments in the eight parameters to identify the lowest local minimum possible. This will be discussed more later.

To summarize, this procedure constructs a practical, two-burn, low-energy lunar transfer between a specified Earth departure and a specified lunar arrival. The altitude, eccentricity, and inclination of the Earth parking orbit are specified and fixed, as is the date of the trans-lunar injection maneuver. The target lunar orbit, the LOI position, and the LOI date are all specified and fixed. The TLI maneuver is constrained to be tangential to the parking orbit, though the orientation of the parking orbit may vary; the LOI maneuver is not constrained to be tangential. Finally, the dates of two trans-lunar maneuvers are permitted to vary, which therefore changes their  $\Delta V$  values.

To illustrate this entire targeting process, Table 6-4 tracks the eight control variables that have been used to generate the adjusted trajectory shown in Figs. 6-2 and 6-3. That is, Table 6-4 shows the steps that were taken to adjust the trajectory from the reference ballistic transfer, which has an Earth departure inclination of 38.3 deg on April 1, 2010, to the desired transfer, which has an Earth departure inclination of 28.5 deg on April 2, 2010. The reference trajectory is summarized in Step 1: the only control variables set are the components of the LOI  $\Delta V$ . Step 2 does not change any control variables and is hence not shown. Step 3 illustrates the small change in the components of the LOI  $\Delta V$  vector that are required to shift the timing of the trajectory's perigee from April 1, 2010 to April 2, 2010, coinciding with the TLI maneuver, though the perigee altitude is now 5200 km. The adjustment amounts to a difference of only 3.3 centimeter per second (cm/s) in the LOI  $\Delta V$  magnitude. Steps 4–6 construct initial guesses for the departure parameters and place two deterministic maneuvers en route to construct a complete end-to-end trajectory. Finally, Step 7 includes the full optimization, where all eight parameters are permitted to vary and the transfer  $\Delta V$  is minimized.

During Step 4, initial guesses for  $\Omega_{\text{TLI}}$  and  $\nu_{\text{TLI}}$  are needed. In this example they are both set to 0 deg; however, it has been observed that the entire procedure may converge to different local minima using different combinations of initial guesses for these parameters. There are often two local minima that correspond to the typical *short* and *long* coasts for the Earth departure. In addition, the process often converges on different local minima depending on the propagation duration of the initial Earth departure. Research indicates that it is typically computationally efficient to perform Steps 4–6 numerous times with different initial guesses and then send only the best one or two trajectories into Step 7 [190, 191]. This process ensures that the majority of local minima are explored without spending too much time in Step 7, which is by far the most computationally demanding step. It is likely that additional small improvements may be made, but this procedure generates a reliable estimate of the minimum transfer  $\Delta V$  given a reference lunar transfer.

Taking the preceding into account, this targeting algorithm yields a trajectory that requires only 24.1 m/s of deterministic  $\Delta V$  to compensate for the change in departure inclination and departure date. This deterministic  $\Delta V$  will vary throughout a full launch period, but this is a small  $\Delta V$  penalty compared to the cost of launching into parking orbits at widely varying inclinations.



**Table 6-4** The history of the example lunar transfer's control variables as the mission is constructed, where  $\Delta t_{\text{TCM1}}$  is the duration of time between TLI and TCM1 and  $\Delta t_{\text{TCM2}}$  is the duration of time between TCM1 and TCM2 [190] (Copyright © 2012 by American Astronautical Society Publications Office, San Diego, California (Web Site: <http://www.univelt.com>), all rights reserved; reprinted with permission of the AAS).

Step #	TLI Parameters			TCM1		TCM2		LOI $\Delta V_x$ , $\Delta V_y$ , and $\Delta V_z$ m/s, EME2000	Total Transfer $\Delta V$ , m/s
	$\Omega$ deg	$\nu$ deg	$\Delta V$ m/s	$\Delta t$ days	$\Delta V$ m/s	$\Delta t$ days	$\Delta V$ m/s		
1	-	-	-	-	-	-	-	-87.728, -271.090, -583.108	-
3	-	-	-	-	-	-	-	-87.732, -271.103, -583.138	-
4	0.00	0.00	3197.44	-	-	-	-	-87.732, -271.103, -583.138	-
5	-25.00	27.18	3196.77	-	-	-	-	-87.732, -271.103, -583.138	-
6	-25.00	27.18	3196.77	21.00	26.10	34.84	6.37	-87.732, -271.103, -583.138	681.500
7	-25.08	27.32	3196.79	20.63	24.09	34.86	0.00	-87.736, -271.118, -583.167	673.155

### 6.5.4 Building a Launch Period

The process described in 6.5.1 may be repeated for each day in a wide range of dates to identify a practical launch period. The total transfer  $\Delta V$  typically rises as the TLI date is adjusted further from a reference trajectory's TLI date. For the purpose of these studies, a search is conducted that extends 30 days on either side of the reference trajectory's TLI date and the best, practical, 21-day launch period is identified within those 61 days. The 21 days of opportunities do not have to be consecutive, though they are typically collected in either one or two segments. Since low-energy transfers travel beyond the orbit of the Moon, they may interact with the Moon as they pass by, even if they pass by at a great distance. The Moon may boost or reduce the spacecraft's energy as it passes by, depending on the geometry; typically there is a point in a launch period where the geometry switches and it is often beneficial to avoid launching on one or several days when the geometry is not ideal.

Figure 6-6 illustrates the transfer  $\Delta V$  cost required to target the reference lunar transfer studied in the previous section as a function of TLI date. Each transfer has been generated using the procedure outlined previously, but with a different TLI date. The trajectories that launch 5–6 days prior to the reference transfer are significantly perturbed by the Moon, though not perturbed enough to break the launch period into two segments. This perturbation is also visible in Fig. 6-4, where a sudden change in the geometry of the transfers appears. One can see that the least expensive 21-day launch period requires a transfer  $\Delta V$  of approximately 706.2 m/s.

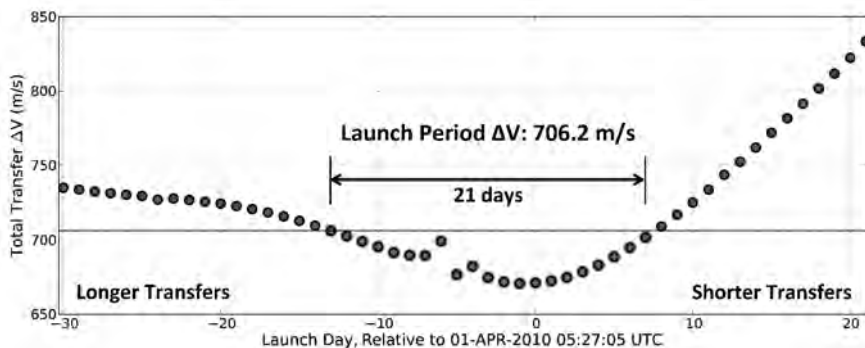


**Figure 6-6** An example 21-day launch period, constructed using the reference lunar transfer presented in Fig. 6-1 [190] (Copyright © 2012 by American Astronautical Society Publications Office, San Diego, California (Web Site: <http://www.univelt.com>), all rights reserved; reprinted with permission of the AAS).

### 6.5.5 Reference Transfers

A total of 288 reference transfers have been used to generate lunar missions with realistic, 21-day launch periods, each starting from a 28.5-deg LEO parking orbit. These reference trajectories have been randomly sampled from low- $\Delta V$ , simple, low-energy transfers presented in the surveys found in Section 4.4. The trajectories target low lunar orbits with any longitude of ascending node and with any argument of periapsis, though the combination of those parameters must yield a satisfactory reference transfer. The transfers arrive at the Moon at any of eight arrival times evenly distributed across a synodic month between July 11, 2010 at 19:41 UTC and August 6, 2010 at 20:37 UTC. The majority of the reference transfers sampled here implement lunar orbit insertion maneuvers with magnitudes between 640 m/s and 750 m/s, though reference transfers have been sampled with LOI  $\Delta V$  values as high as 1080 m/s. These  $\Delta V$  values correspond with the full cost of capturing and reducing the orbit to a 100-km circular orbit; although that process typically involves many maneuvers, in this study it will be performed by one maneuver. Finally, reference transfers have been sampled with transfer durations between 65 and 160 days. This collection of reference transfers makes no assumptions about what sort of mission a designer may be interested in, except that each transfer is simple, that is, it includes no Earth-phasing orbits nor lunar flybys, and each transfer targets a polar lunar orbit.

### 6.5.6 Statistical Costs of Desirable Missions to Low Lunar Orbit

In general, the algorithms described in this section generate successful launch periods with similar characteristics. Figure 6-7 illustrates the total transfer  $\Delta V$  of several example launch periods that have been generated from these reference transfers. One notices that many of these launch periods include a single main convex  $\Delta V$  minimum, from which a 21-day launch period is easily identified. Other  $\Delta V$  curves include two or more local minima. The launch periods are designed to have at most two gaps, where each gap must be less than 14 days in extent. A particular lunar mission may have different requirements dictating the breadth of each segment and/or gap, which will likely change the launch period's cost; the requirements used here are simply representative of a real mission.

It has been found that most 21-day launch periods among the 288 missions studied include the reference launch date, though there are many examples that do not, including two of those shown in Fig. 6-7. In some cases a practical launch period may have extended further than 30 days from the reference launch date and required less total  $\Delta V$ . A particular lunar mission may certainly relax this constraint, but these extended launch periods are not explored here in order to keep the constraints consistent across every mission studied.

Once again, one also sees frequent lunar perturbations in the 288 launch periods studied, much like the example launch period shown in Section 6.5.4. Since each transfer in a particular launch period departs the Earth in approximately the same direction, the Moon passes near the transfer's outbound leg about once every synodic

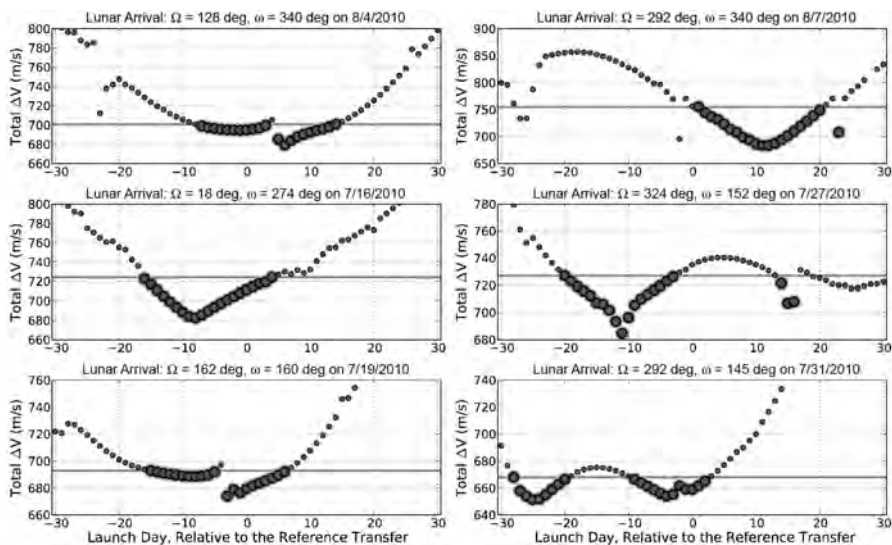


**Figure 6-7** Several example curves that illustrate the post-TLI  $\Delta V$  cost of transferring from a 28.5-deg LEO parking orbit at different TLI dates to a given reference low-energy transfer, including a highlighted 21-day launch period in each case [190] (Copyright © 2012 by American Astronautical Society Publications Office, San Diego, California (Web Site: <http://www.univelt.com>), all rights reserved; reprinted with permission of the AAS).

month. This causes a brief jump in the launch period. Some transfers do not experience any significant perturbations due to their out-of-plane motion.

Figures 6-8 and 6-9 illustrate two additional views of the six example launch periods shown in Fig. 6-7. Figure 6-8 shows the view of each trajectory in each of the six launch periods as if viewed from above the ecliptic in the Sun–Earth rotating frame, such that the Sun is toward the left in each plot. One notices that some of these launch periods traverse toward the Sun and others traverse away from the Sun. The transfers arrive at the Moon at the exact same point in each mission, but each mission arrives at the Moon at different points in its orbit. The reference transfers are sampled randomly to include a wide variety of different target lunar orbit geometries, arrival times, and transfer durations. Figure 6-9 illustrates the profile of a spacecraft's distance from the Earth over time while traversing each trajectory in each of the six launch periods. One can see that each design involves trajectories with different transfer durations, and trajectories that traverse to different maximum distances. The optimization processes often shift the epochs of the trajectory correction maneuvers, though one can see that the TCM epochs are sometimes shifted more on one trajectory than on its neighbors, depending on the sensitivity of that variable on the trajectory's  $\Delta V$  costs. Similarly, some TLI parameters are shifted more in one trajectory than its

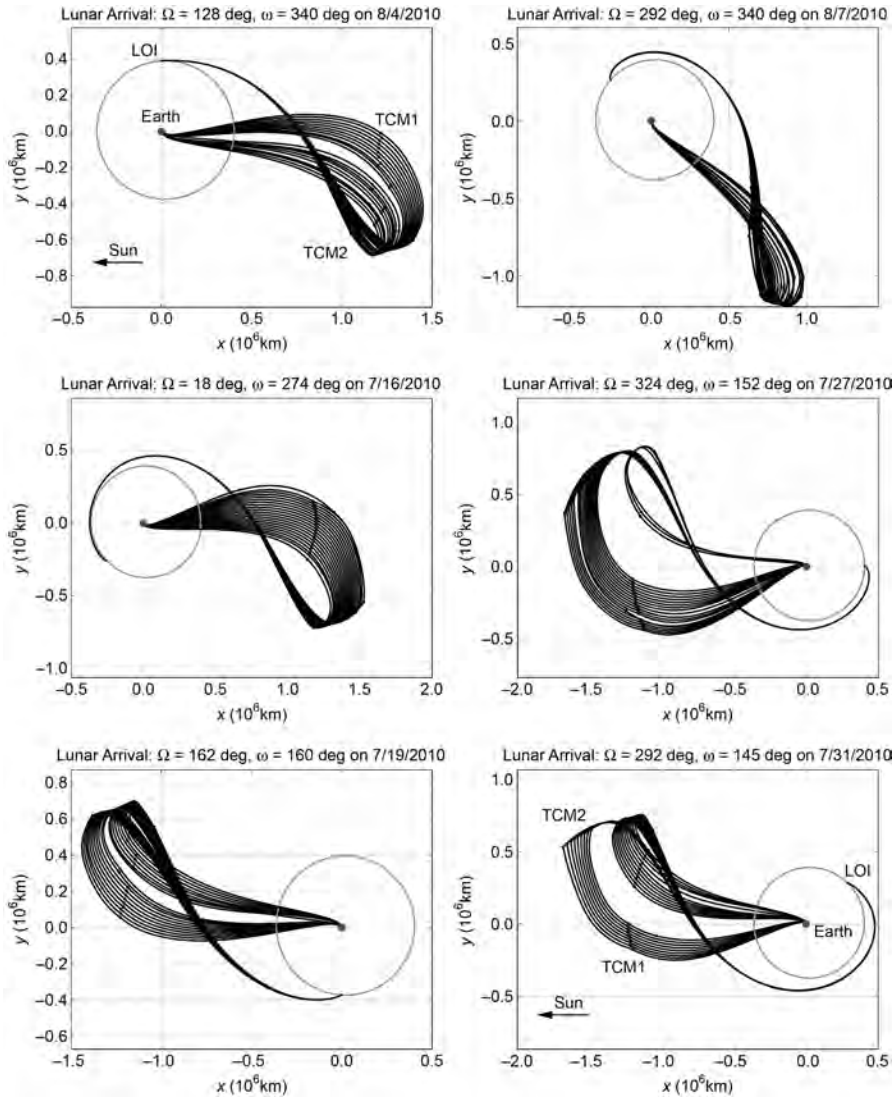


**Figure 6-8** Each trajectory in each of the six launch periods illustrated in Fig. 6-7, viewed from above the ecliptic in the Sun–Earth rotating frame. The Moon’s orbit is shown for reference.

neighbors. It is likely that a mission designer would use these results to guide further refinements in the optimization of a real mission.

The examples shown in Figs. 6-7–6-9 illustrate six missions; the remainder of this discussion focuses on the random sample of 288 similar missions. Figure 6-10 shows

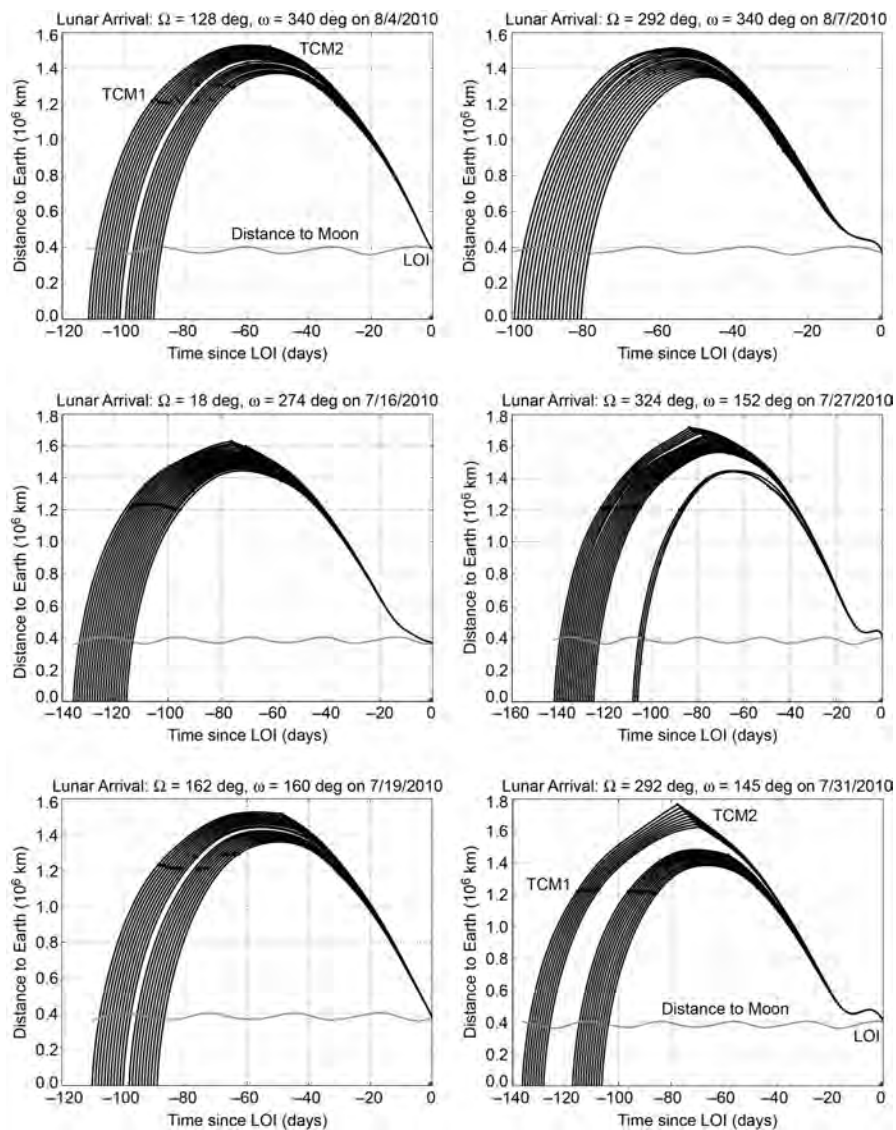


**Figure 6-9** The distance from Earth over time for each transfer in the six launch periods shown in Figs. 6-7 and 6-8. The distance to the Moon over time is shown for reference.

the range of the transfer  $\Delta V$  values that are contained in each 21-day launch period in these 288 missions as a function of their reference transfer  $\Delta V$ . As an example, the launch period illustrated in Fig. 6-6 was generated using a reference transfer with

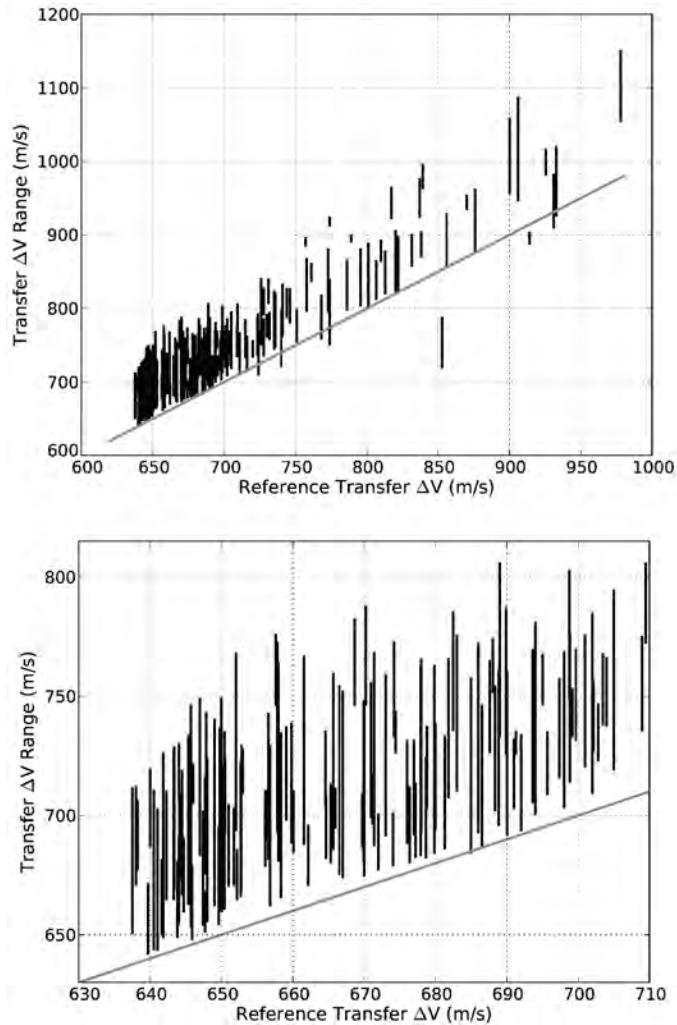


**Figure 6-10** The range of transfer  $\Delta V$  values contained in each 21-day launch period as a function of the reference transfer  $\Delta V$  shown in normal view (top) and exploded view (bottom) [190] (Copyright © 2012 by American Astronautical Society Publications Office, San Diego, California (Web Site: <http://www.univelt.com>), all rights reserved; reprinted with permission of the AAS).

a  $\Delta V$  of 649 m/s (the ordinate of the plots in Fig. 6-10), and the resulting launch period included missions that had transfer  $\Delta V$  values between 670.6 and 706.2 m/s. One can see that the majority of transfers studied here have reference transfer  $\Delta V$  values less than 750 m/s, though the transfers sampled include those with reference  $\Delta V$  values as great as 1080 m/s. The launch period  $\Delta V$  range often starts above the

mission's reference  $\Delta V$ , since each mission starts from a 28.5-deg LEO parking orbit and the reference transfer typically departs from some other inclination. In a few cases, and one extreme case, the launch period  $\Delta V$  range starts below the reference  $\Delta V$ . This is often possible when the reference transfer has a natural Earth departure far from 28.5 deg and a change in the transfer duration reduces the total  $\Delta V$ . The plots in Fig. 6-10 clearly illustrate that the  $\Delta V$  cost of establishing a 21-day launch period is highly dependent on the reference transfer's total  $\Delta V$ . The launch period  $\Delta V$  cost of these 288 example transfers requires approximately  $71.67 \pm 29.71$  m/s ( $1\sigma$ ) more deterministic  $\Delta V$  than the transfer's reference  $\Delta V$ .

The launch periods studied here include missions that depart the Earth on 21 different days, and the launch period  $\Delta V$  cost is the  $\Delta V$  of the most expensive transfer in that set. The departure days do not need to be consecutive, as described earlier. In general, increasing the number of launch days included in a launch period increases the  $\Delta V$  cost of the mission. Figure 6-11 shows a plot of the change in the launch period  $\Delta V$  cost of the 288 missions studied here as one adds more days to each mission's launch period, relative to the case where each mission has only a single launch day. The line of best fit through these data indicates that on average it requires approximately 2.480 m/s per launch day to add days to a mission's launch

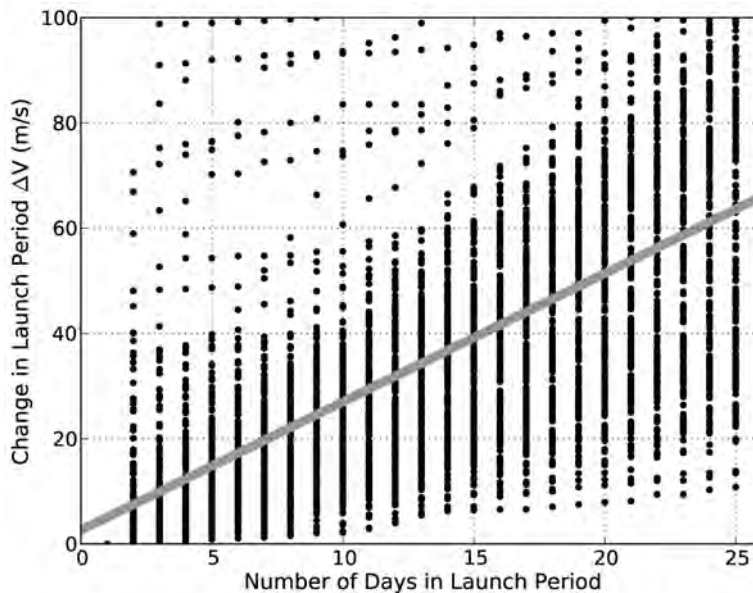


**Figure 6-11** The change in the launch period  $\Delta V$  cost of the 288 missions studied here as a function of the number of days in the launch period. The linear trend has a slope of 2.480 m/s per launch day [190] (Copyright © 2012 by American Astronautical Society Publications Office, San Diego, California (Web Site: <http://www.univelt.com>), all rights reserved; reprinted with permission of the AAS).



period. There is a significant jump in the launch period  $\Delta V$  when one moves from a 1-day launch period to a 2-day launch period. This is due to the fact that the Moon's perturbations often produce a single launch day with remarkably low  $\Delta V$  requirements. The change in a launch period's required  $\Delta V$  would be more smooth if the effects of lunar perturbations on the Earth-departure leg were ignored.

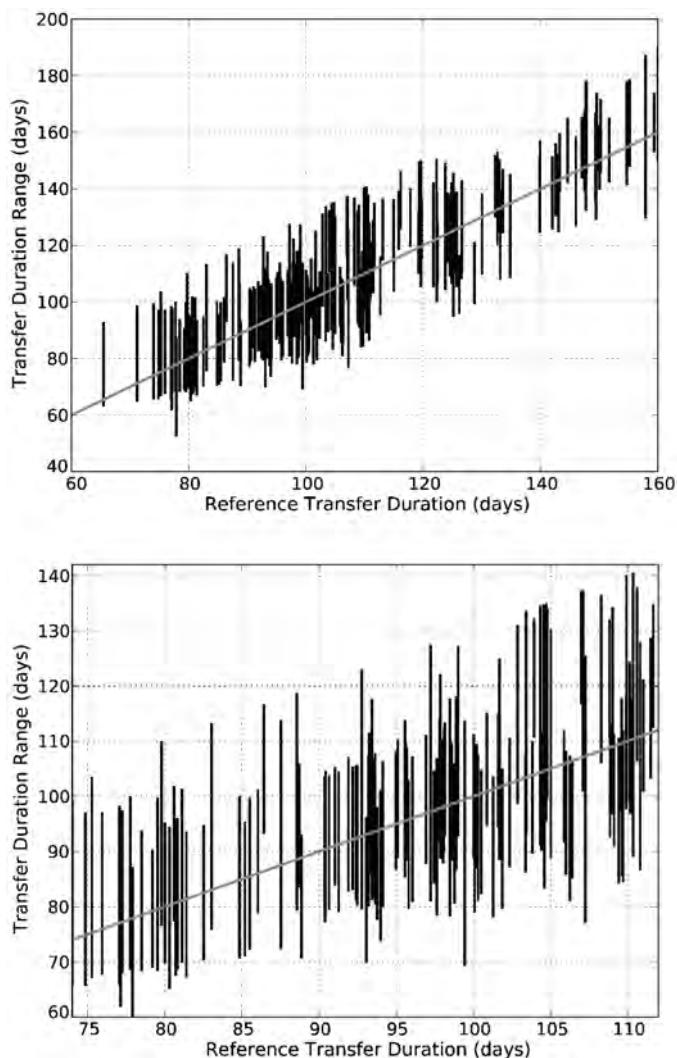
It has been noted, when studying Fig. 6-7, that a launch period does not necessarily include the reference launch date. However, it is expected that the transfer duration of a reference trajectory may be used to predict a mission's actual transfer duration. Figure 6-12 tracks the range of transfer durations within each 21-day launch period studied here as a function of the mission's reference transfer duration. One can see that the range of transfer durations is indeed correlated with the reference transfer duration. Furthermore, it has been found that the maximum transfer duration of the 288 launch periods is approximately  $15.95 \pm 8.66$  days longer than the mission's reference duration, the minimum transfer duration is approximately  $10.91 \pm 7.75$  days shorter than the reference duration, and the total number of days between the first and final launch date of a given launch period may be estimated at approximately  $26.86 \pm 6.95$  days. Hence, one may predict that a mission's launch period will include 21 of about 27 days, centered on a date several days earlier than the reference launch date, if one constructs a 21-day launch period using the same rules invoked here.

Figure 6-13 tracks the range of  $\Delta V$  costs associated with each launch period as a function of the duration of the mission's reference transfer. One can see that there is a wide spread of transfer  $\Delta V$  across the range of durations. As the reference transfer duration drops below 90 days, the launch period  $\Delta V$  cost climbs, which makes sense because there is less time to perform maneuvers during the shorter transfers. Beyond 90 days, there are launch periods with low  $\Delta V$  requirements for any transfer duration.

It is expected that the launch period's  $\Delta V$  cost is dependent upon the reference transfer's natural Earth departure inclination. It is hypothesized that a reference transfer that departs the Earth with an inclination near 28.5 deg will generate a launch period that requires less total  $\Delta V$  than a reference transfer that departs the Earth with a far different inclination. Figure 6-14 tracks the launch period  $\Delta V$  cost of the 288 missions constructed here as a function of their reference departure inclination values. The bottom plot in Fig. 6-14 observes the range of transfer  $\Delta V$  values as a function of the difference between the reference departure inclination value and the target 28.5-deg value. A line has been fit to the maximum  $\Delta V$  for each launch period using a least-squares approach, which yields the relationship:

$$\text{Launch Period } \Delta V \sim (0.470 \text{ m/s/deg}) \times x + 756.5 \text{ m/s}$$

where  $x$  is equal to the absolute value of the difference between the reference departure inclination and 28.5 deg. The sample set of lunar transfers includes low- $\Delta V$  and high- $\Delta V$  missions, which may swamp any significant relationship between the launch period's  $\Delta V$  cost and the reference departure inclination. Nevertheless, it is very interesting to observe that the launch period's  $\Delta V$  cost does not present a strong correlation with the reference departure inclination.



**Figure 6-12** The range of transfer durations contained in each 21-day launch period as a function of the reference transfer duration. The plot at the bottom shows an exploded view, focused on transfer durations between 75 and 115 days [190] (Copyright © 2012 by American Astronautical Society Publications Office, San Diego, California (Web Site: <http://www.univelt.com>), all rights reserved; reprinted with permission of the AAS).

To further test the relationship of a launch period to the reference LEO inclination, each launch period's  $\Delta V$  has been reduced by its reference  $\Delta V$  so that each launch period may be more closely compared. Figure 6-15 shows the same two plots as

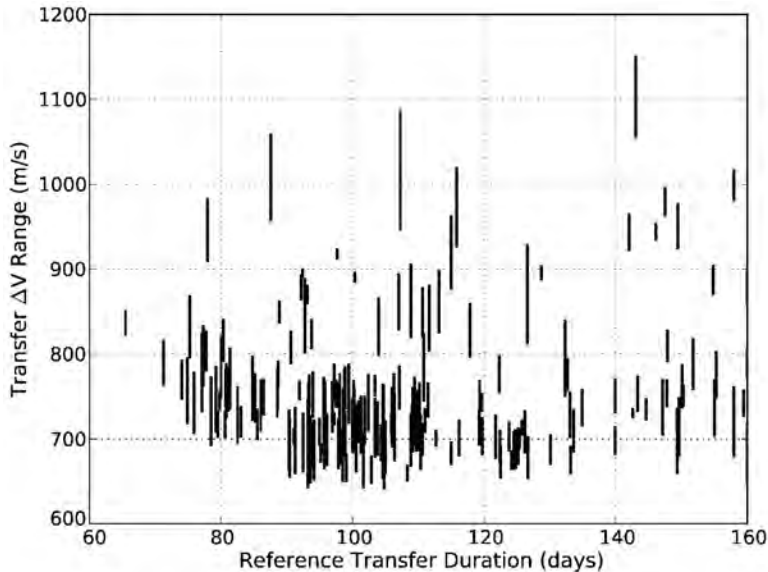


**Figure 6-13** The range of transfer  $\Delta V$  costs contained in each 21-day launch period as a function of the reference transfer's duration [190] (Copyright © 2012 by American Astronautical Society Publications Office, San Diego, California (Web Site: <http://www.univelt.com>), all rights reserved; reprinted with permission of the AAS).

shown in Fig. 6-14, but with each mission's reference  $\Delta V$  subtracted from its launch period  $\Delta V$  range. One can see that the launch period  $\Delta V$  is not well correlated with the reference departure inclination. The linear fit has a slope of only 0.206 m/s per degree of inclination away from 28.5 deg. It appears that a 21-day launch period absorbs most of the  $\Delta V$  penalty associated with inclination variations. The natural Earth departure inclination of a transfer certainly varies with transfer duration, and it has already been noticed that the launch period is often not centered about the reference transfer's TLI date. This result is useful, because it indicates that the natural Earth departure inclination is not a good predictor of the launch period  $\Delta V$  requirement of a reference transfer. The relationship of the low-energy transfer  $\Delta V$  and the TLI inclination is further explored in the next section.

### 6.5.7 Varying the LEO Inclination

The results presented previously in this section have only considered missions that begin in a LEO parking orbit at an inclination of 28.5 deg relative to the Equator, corresponding to launch sites such as Cape Canaveral, Florida. Spacecraft missions certainly depart the Earth from other launch sites; launch vehicles from those sites typically deliver the most mass to low Earth orbit if they launch into a parking orbit at an inclination approximately equal to their launch site's latitude. Hence, it

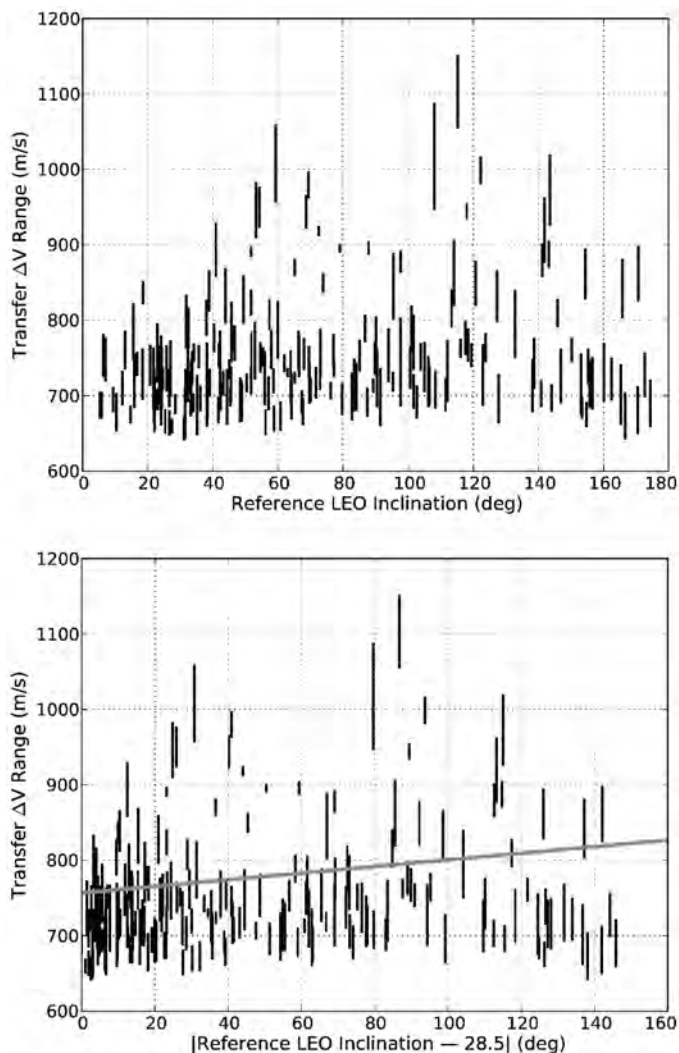


**Figure 6-14** The range of transfer  $\Delta V$  costs contained in each 21-day launch period as a function of the reference transfer's Earth departure inclination (top) and the absolute value of the difference between the reference inclination and 28.5 deg (bottom) [190] (Copyright © 2012 by American Astronautical Society Publications Office, San Diego, California (Web Site: <http://www.univelt.com>), all rights reserved; reprinted with permission of the AAS).

is of interest to determine the  $\Delta V$  cost required to depart the Earth from any LEO inclination and transfer to the same lunar orbit using a particular low-energy reference transfer.

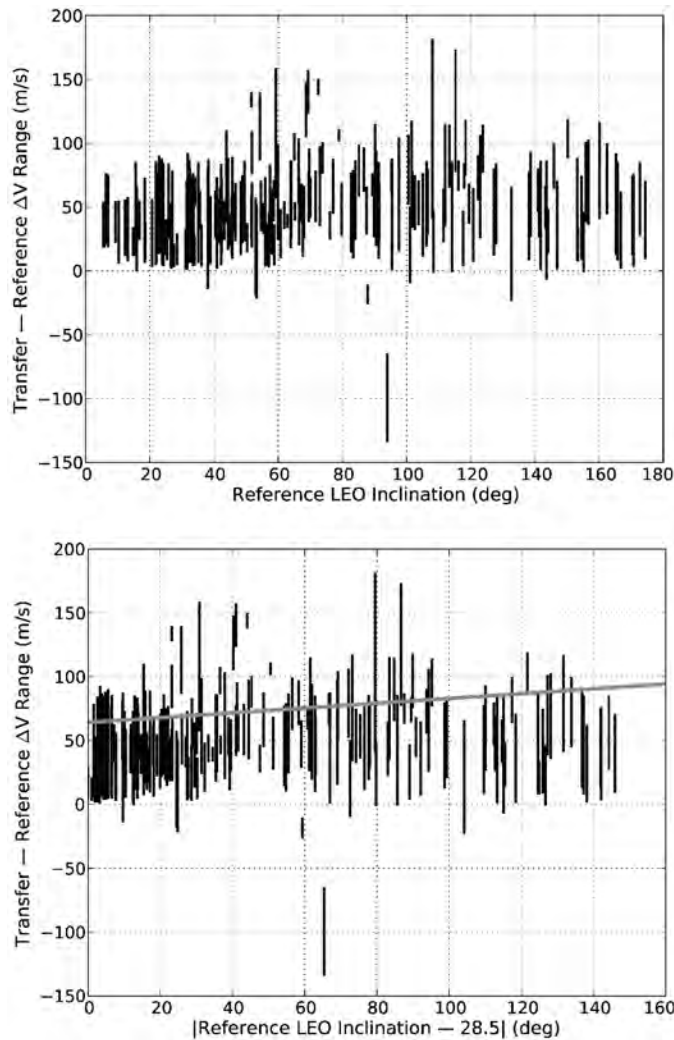


**Figure 6-15** The same two plots as shown in Fig. 6-14, but with each mission's reference  $\Delta V$  subtracted from its 21-day launch period  $\Delta V$  range [190] (Copyright © 2012 by American Astronautical Society Publications Office, San Diego, California (Web Site: <http://www.univelt.com>), all rights reserved; reprinted with permission of the AAS).

The algorithms described here have been used to generate missions that depart the Earth from LEO parking orbits at a wide range of inclinations and then target the same reference low-energy transfer discussed earlier (described in Section 6.5.2 and illustrated in Fig. 6-1). The reference trajectory naturally departs the Earth on April 1, 2010, from an orbital inclination of approximately 38.3 deg; hence, a mission

that departs the Earth at that time from that orbit requires no deterministic maneuvers en route to the Moon. Upon arrival at the Moon, the reference trajectory requires a 649.0-m/s orbit insertion maneuver to impulsively enter the desired 100-km circular lunar orbit. Any mission that departs the Earth from a different inclination will require deterministic TCMs and/or a different orbit insertion maneuver.

Figure 6-16 illustrates how the deterministic  $\Delta V$  varies for missions that depart the Earth at different LEO inclination values and target the same lunar orbit. The dates and times of the trans-lunar injection and lunar orbit insertion are fixed. The total transfer  $\Delta V$  is shown on the top, and the difference between each mission's total  $\Delta V$  compared to the reference transfer's total  $\Delta V$  is shown on the bottom. One can see that the  $\Delta V$  cost of the mission rises as a function of the difference between the mission's departure inclination and the reference transfer's departure inclination. The cost is approximately 0.97 m/s per degree of inclination change for missions with LEO inclinations greater than 20 deg. The transfer cost increases much more rapidly as a mission's departure approaches equatorial. As the departure inclination drops, the system gradually loses a degree of freedom: the LEO parking orbit's ascending node becomes less influential on the geometry of the departure. The ascending node is no longer defined for equatorial departures, and the lunar transfer requires greater than 120 m/s more deterministic  $\Delta V$  than the reference transfer.

As Fig. 6-16 illustrates, the total  $\Delta V$  of a mission to the reference lunar orbit is minimized if the LEO parking orbit has an inclination of 38.3 deg, provided that the trans-lunar injection is performed on April 1, 2010. If the TLI date is shifted, then the optimal LEO inclination is likely to shift as well. Hence, the  $\Delta V$  cost of a full 21-day launch period cannot be strictly predicted by observing the difference in inclination between a desired LEO parking orbit and the reference departure.

Figure 6-17 illustrates three launch periods, corresponding to missions that depart from LEO parking orbits with inclinations of 20, 50, and 80 deg. One can see that the launch period shifts in time, illustrating that the transfer duration may significantly alter the reference trajectory's natural departure inclination. Figure 6-18 illustrates the total transfer  $\Delta V$  for each launch opportunity of a 21-day launch period departing from a wide range of departure inclinations. One can see that the launch period  $\Delta V$  is dramatically higher for low inclinations and that the  $\Delta V$  changes very little from one inclination to another for higher inclination values. It is interesting that the missions with higher inclinations require less  $\Delta V$  than missions near the reference transfer's departure inclination. The low- $\Delta V$  points in the lower left part of the plot correspond to brief opportunities in those launch periods when the Moon passes through an ideal location in its orbit to reduce the transfer  $\Delta V$ .

### 6.5.8 Targeting a Realistic Mission to Other Destinations

The algorithms presented in Section 6.5.3 have been applied to the problem of constructing realistic missions to low lunar orbit. The algorithms require little modification for missions to other destinations, such as lunar libration orbits or the lunar surface.

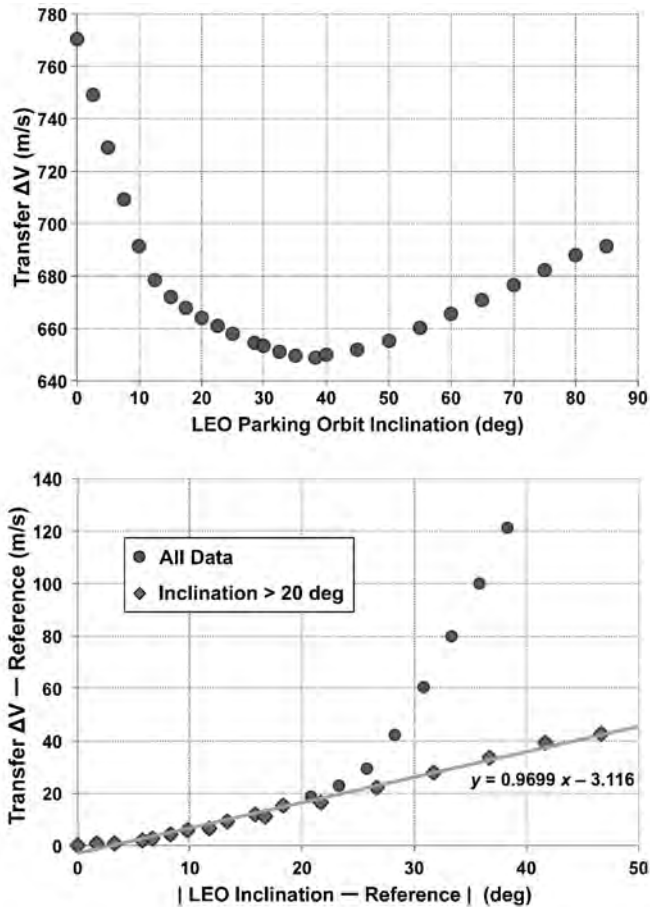


**Figure 6-16** How deterministic  $\Delta V$  varies for different LEO inclination values. Top: The total transfer  $\Delta V$  for missions that depart the Earth on April 1, 2010, at different inclinations and arrive at the same reference lunar orbit. Bottom: The difference in the total transfer  $\Delta V$  for these missions compared with the reference low-energy transfer, which departs at an inclination of  $\sim 38.3$  deg [190] (Copyright © 2012 by American Astronautical Society Publications Office, San Diego, California (Web Site: <http://www.univelt.com>), all rights reserved; reprinted with permission of the AAS).

*Missions to the Lunar Surface.* Certainly a mission to the lunar surface may first target an intermediate lunar orbit, such as a low lunar orbit or a lunar libration orbit. Intermediate orbits provide some risk-reduction in the case of a contingency, because one may postpone the landing until the system is fully prepared to land. Alternatively, one may construct a mission that is designed to land immediately upon arrival at the Moon, with the option to divert into a parking orbit of some kind in the event of a

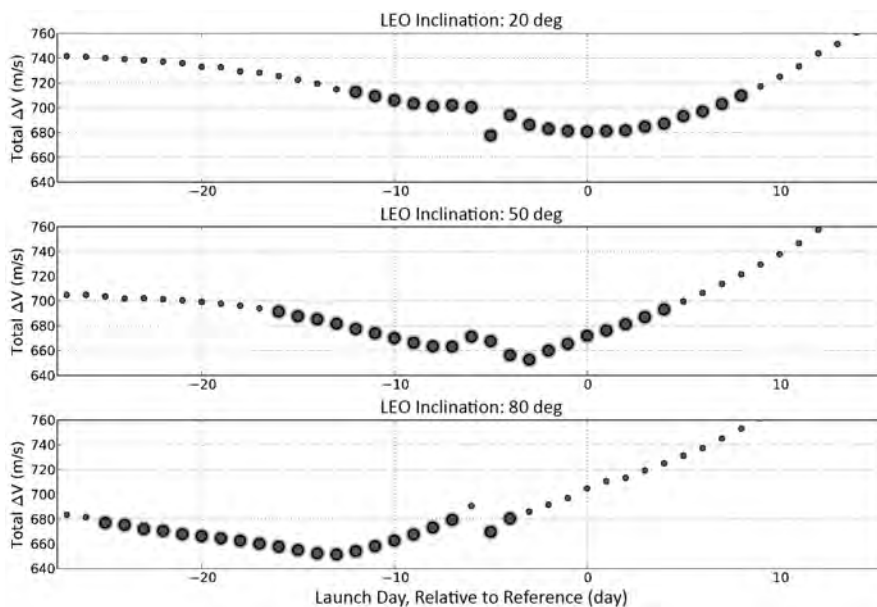


**Figure 6-17** Three launch periods for missions to the reference lunar orbit, where each launch period is designed to accommodate a specific LEO inclination; namely, 20 deg (top), 50 deg (middle), and 80 deg (bottom). The Moon perturbs the outbound trajectories for those missions that launch about 5 days before the reference transfer [190] (Copyright © 2012 by American Astronautical Society Publications Office, San Diego, California (Web Site: <http://www.univelt.com>), all rights reserved; reprinted with permission of the AAS).

contingency. In this scenario, or in the scenario where the mission design has no option but to land immediately, the targeting algorithms described in Section 6.5.3 may be easily modified to accommodate a lander instead of an orbiter.

A lander may be able to adjust its time of arrival or its incoming velocity magnitude, flight path angle, or flight path azimuth. If these parameters must be held fixed, for example, to reduce the complexity, risk, or cost of the design, then one may instead introduce a third trajectory correction maneuver, performed some significant amount of time prior to landing, in order to minimize the total launch period  $\Delta V$ .

**Missions to Lunar Libration Orbits.** There are many reasons why a mission to a lunar libration orbit, or other three-body orbit, would benefit by designing a single libration orbit and constructing a launch period that inserted the spacecraft into that same libration orbit. For instance, a mission design team building a lunar lander and/or sample return mission may be interested in focusing their efforts to validate one specific landing sequence, and would have to spend a great deal more effort to support 21 different landing sequences, with varying geometry and timing. It may therefore be less expensive and more reliable to implement a mission that targets



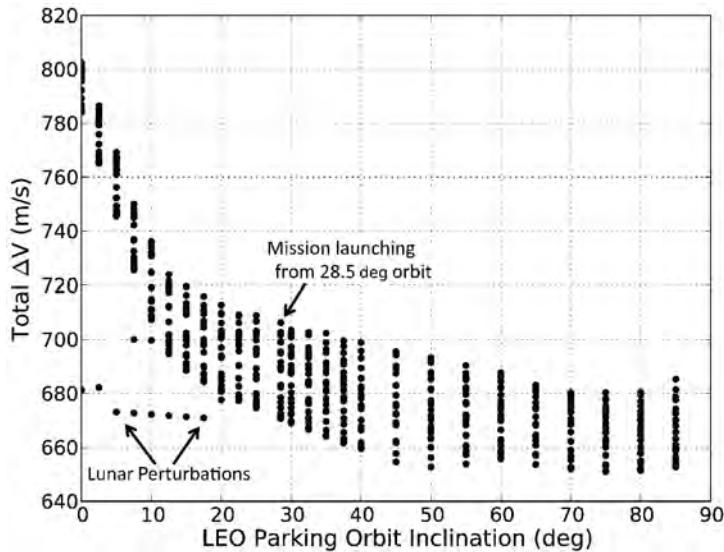


**Figure 6-18** The total transfer  $\Delta V$  for each opportunity of a 21-day launch period for missions to the reference lunar orbit, departing from LEO parking orbits with varying inclination values [190] (Copyright © 2012 by American Astronautical Society Publications Office, San Diego, California (Web Site: <http://www.univelt.com>), all rights reserved; reprinted with permission of the AAS).

a particular lunar libration orbit, no matter which day it launches on, even if that mission design required slightly higher  $\Delta V$  budget.

Studies have demonstrated that the algorithms presented here may be used very successfully in conjunction with a libration orbit insertion maneuver [183, 184].

### 6.5.9 Launch Period Design Summary

The goal of this section is to characterize the  $\Delta V$  costs associated with building a 21-day launch period for a practical mission to the Moon via a low-energy transfer. We have sampled 288 different low-energy transfers between the Earth and polar orbits about the Moon and have constructed practical 21-day launch periods for each of them, using a 28.5-deg LEO parking orbit and no more than two deterministic maneuvers. The lunar orbits have a wide range of geometries, though they are all polar and have an altitude of approximately 100 km. The reference low-energy transfers include no Earth-phasing orbits nor close lunar flybys, and they require between 65 and 160 days of transfer duration. Each mission has been constructed by using a sequence of steps, varying eight parameters to minimize the transfer  $\Delta V$  cost. The eight variable parameters include the parking orbit's ascending node, the trans-lunar injection's location in the parking orbit, the trans-lunar injection's  $\Delta V$ , the

times of two deterministic maneuvers en route to the Moon, and three components of the lunar orbit insertion maneuver. All other aspects of the transfer are fixed when building a particular mission.

Several conclusions may be easily drawn from the results presented here. First of all, the cost of a launch period is obviously dependent on the number of launch days in the period. The transfers constructed here demonstrate that it costs on average approximately 2.5 m/s per day added to a launch period; hence, the average 21-day launch period requires about 50 m/s more deterministic  $\Delta V$  than a 1-day launch period for a given transfer. The cost of a particular launch period may rise nonlinearly as one adds days to the launch period, such that it may be the case that additional days cost exponentially more  $\Delta V$  or perhaps that additional days do not cost any additional  $\Delta V$ . The statistical cost of establishing a 21-day launch period to the 288 reference transfers studied in this section is approximately  $71.7 \pm 29.7$  m/s ( $1\sigma$ ), where the additional  $\Delta V$  of more than the 50 m/s is required to accommodate a departure from a 28.5-deg LEO parking orbit. The 21 opportunities in the launch period may be on 21 consecutive days, and frequently are, but typically include one or two gaps. The average launch period for these 288 missions requires a total of 27 days; the vast majority of the launch periods may be contained within 40 days. Finally, we have shown that there is no significant trend between the total launch period  $\Delta V$  for these 288 missions and their reference departure inclination values or their reference transfer durations, except for short transfers with durations below 90 days.

An additional study has been performed to observe how a mission's  $\Delta V$  changes as a function of the particular LEO inclination selected. A mission that departs at a particular time requires approximately 0.97 m/s more transfer  $\Delta V$  per degree of inclination change performed, assuming that the departure inclination is greater than 20 deg. The total transfer  $\Delta V$  cost increases dramatically as the departure inclination approaches 0 deg. These trends change when considering a full 21-day launch period. The required launch period  $\Delta V$  is still high for missions that depart from nearly equatorial LEO parking orbits, but the variation in the launch period  $\Delta V$  is reduced for missions that depart at higher inclinations.

## 6.6 NAVIGATION

Spacecraft traversing low-energy lunar transfers may be navigated in very similar fashions to those following interplanetary transfers. Indeed, there are many similarities: the trajectories require many weeks, they traverse well beyond the orbit of the Moon, they require trajectory correction maneuvers, etc. There are several differences, including the fact that low-energy lunar transfers remain captured by the Earth, they are not well-modeled by conic sections, and they are unstable. This section discusses how these similarities and differences impact the navigation and operation of the spacecraft during such transfers.

### 6.6.1 Launch Targets

Launch vehicle operators typically target three parameters when injecting spacecraft onto interplanetary trajectories: one describing the target energy, namely,  $C_3$ , and two angular measurements describing the orientation of the departure asymptote, namely, the right ascension and declination of the launch asymptote, RLA and DLA, respectively. Low-energy lunar transfers, conversely, remain captured by the Earth and do not have launch asymptotes. The GRAIL project used two similar target parameters to describe the orientation of the departure ellipse—the right ascension and declination of the instantaneous apogee vector (RAV and DAV, respectively) at the time of the launch vehicle’s target interface point (TIP). Combined with the target  $C_3$  parameter, these three targets describe a departure that keeps the expected correction  $\Delta V$  after the TIP to a minimum.

### 6.6.2 Station-Keeping

As illustrated in Chapter 2, low-energy lunar transfers are unstable; they depend on a careful balance of the gravitational attraction of the Sun, Earth, and Moon. Any random deviation from the designed trajectories will grow exponentially over time. Therefore, a spacecraft traversing a low-energy lunar transfer in the presence of realistic uncertainties will require TCMs to remain on a desirable course. Fortunately, low-energy lunar transfers are stable enough that maneuvers are typically only needed every 4–8 weeks, though more are needed to support any lunar approach and/or lunar flybys.

The cost of performing statistical corrections on a low-energy lunar transfer may be estimated by considering the stability of trajectories in each region of space that the transfer passes through. First, typical spacecraft missions plan to perform a maneuver soon after the trans-lunar injection in order to clean up any injection errors. For instance, the GRAIL mission planned to have both spacecraft perform a maneuver within a week after injection. Next, the spacecraft spend 1–3 months traversing a region of space far from the Earth, typically near the Sun–Earth  $L_1$  or  $L_2$  points. The stability of this portion of the trajectory may be approximated by measuring the stability of typical Sun–Earth libration orbits—as illustrated in Section 3.4.1. As the spacecraft approach the Moon either for a lunar flyby or for their final lunar approach, the trajectories become more unstable. The stability of the trajectories near the Moon may be approximated by measuring the stability of typical Earth–Moon libration orbits.

There are many ways to measure the stability of a trajectory, but a rather intuitive way is to consider the trajectory’s *perturbation doubling time*, that is, the amount of time it takes for a spacecraft to double its distance away from a reference trajectory (see Section 2.6.8.3 on page 80). If at time  $t_0$  a spacecraft is 100 km away from its reference trajectory, then at time  $t_0 + \hat{\tau}$  the spacecraft will be approximately 200 km away from its reference, and at time  $t_0 + 2\hat{\tau}$  the spacecraft will be approximately 400 km away from its reference, and so on, where  $\hat{\tau}$  is the perturbation doubling time.

Typical halo orbits about the Sun–Earth  $L_1$  and  $L_2$  points have  $\hat{\tau}$  values of about 17 days. Hence, one may assume that the position error of a spacecraft traversing a low-energy lunar transfer near those orbits will double roughly every  $\sim 17$  days. Fortunately, this is a rather long time for most spacecraft operations unless the spacecraft has particularly strict flight path requirements. The *GRAIL* mission scheduled two trajectory correction maneuvers per spacecraft while they traversed the region of space near  $EL_1$ , though there were deterministic needs for those maneuvers as well. The *Genesis* mission performed maneuvers every couple of months while traversing its  $EL_1$  orbit, requiring only about 10 m/s per year of station-keeping [87]. The *Solar and Heliospheric Observer's (SOHO)* spacecraft has demonstrated the ability to remain in orbit about the  $EL_1$  point for even less  $\Delta V$ . *SOHO*'s first eight station-keeping maneuvers (SKMs) were executed between May 1996 and April 1998, imparting a total  $\Delta V$  of approximately 4.77 m/s: an average of one maneuver per 99 days with an average maneuver  $\Delta V$  of only 0.596 m/s [217].

As a spacecraft approaches the Moon, either for the targeted arrival or for a lunar flyby, its trajectory becomes more unstable and the perturbation doubling time shrinks. If the spacecraft arrives at a lunar libration orbit via a transfer such as those presented in Chapter 3 then its stability may be measured by the perturbation doubling time of typical halo orbits about the Earth–Moon libration points. If the spacecraft's destination is a low lunar orbit, the lunar surface, or a flyby, then this measurement is only an approximation and more analysis is needed. Nevertheless, typical halo orbits about the Earth–Moon  $L_1$  and  $L_2$  points have  $\hat{\tau}$  values of about 1.4 days. Not surprisingly, a spacecraft's position error doubles about twelve times faster in the Earth–Moon system than it does in the Sun–Earth system. Depending on the mission, it may be necessary to perform maneuvers as often as 1–2 times per week to traverse Earth–Moon libration orbits. Even so, the two *Acceleration, Reconnection, Turbulence, and Electrodynamics of the Moon's Interaction with the Sun (ARTEMIS)* spacecraft successfully navigated several months of libration orbits about both the Earth–Moon  $L_1$  and  $L_2$  points, demonstrating that such operations are viable.

There are two fundamentally different strategies that have been implemented when designing the SKMs of historical missions, namely, *tight control* and *loose control*. The term *tight control* describes a strategy where each SKM is designed to bring the spacecraft's trajectory back to a designed reference trajectory. The *International Sun–Earth Explorer-3 (ISEE-3)* and *Genesis* spacecraft maneuvers are good examples of missions that implemented tight station-keeping control [218, 219]. This strategy is used when the spacecraft's trajectory has particular requirements; for the case of *Genesis*, the trajectory ultimately placed the spacecraft on a course to enter the atmosphere for a landing in Utah. Each SKM is designed such that the resulting trajectory intersects the reference trajectory at the time of the next planned SKM. Conversely, a *loose* station-keeping strategy describes one where a spacecraft may travel anywhere within some wide corridor and the particular route taken is not important. For instance, the *SOHO* spacecraft must remain in orbit about the Sun–Earth  $L_1$  point, but the particular path about the  $L_1$  point is not important. Thus, *SOHO*'s trajectory is re-optimized each time an SKM is designed [217]. *SOHO*'s

loose control has resulted in station-keeping  $\Delta V$  costs just over 2 m/s per year, nearly four times lower than *ISEE-3*'s tight station-keeping control costs.

In summary, one may expect to perform a TCM soon after launch in order to clean up injection errors, followed by TCMs every 4–8 weeks when the spacecraft is traversing the cruise phase far from the Earth or Moon, followed by one or two TCMs per lunar approach. If the spacecraft's itinerary includes lunar libration orbits, or other unstable three-body orbits, then one may expect to perform TCMs every 3–7 days during those phases. The total navigation  $\Delta V$  cost depends on the spacecraft and its propulsion system's performance, but it is certainly possible to navigate such trajectories for a modest  $\Delta V$  – on the order of 1–10 m/s per year.

**6.6.2.1 Station-Keeping Strategies** Numerous station-keeping strategies have been formulated since investigators began applying libration orbits to practical spacecraft mission designs [6, 119]. Most developments have been in support of flight projects and proposals that involved trajectories in the Sun–Earth system [218, 220–230]. More recent investigations have examined station-keeping strategies within the Earth–Moon system, especially with the development and success of the *ARTEMIS* mission [17, 186, 231–234]. Folta et al., surveyed a wide variety of station-keeping strategies with the purpose of applying a desirable strategy to the *ARTEMIS* mission [231]. Ultimately, each of the *ARTEMIS* station-keeping maneuvers was designed using a gradient-based optimizer that ensured the spacecraft would remain on the libration orbit for the next few revolutions. This method kept the total station-keeping fuel cost low without requiring the generation of a reference trajectory. After the maneuvers were designed, a later study found that each of the maneuvers closely aligned with the local stable eigenvector at that point of the spacecraft's orbit [235]. This conclusion has certainly prompted researchers to investigate if the stable eigenvector is a good initial guess for a near-optimal station-keeping strategy.

While *ARTEMIS* employed a *loose* station-keeping strategy very successfully, its strategy was focused on the short term: ensuring that the spacecraft remained on a desirable trajectory for the next few revolutions about the Lagrange point. There is concern that any short-term strategy may fail over the long term, resulting in a trajectory that diverges from the desired orbit. Recent work has applied tools such as the multiple-shooting differential corrector to the goal of achieving a minimum- $\Delta V$  long-term station-keeping strategy [234]. This goal is a rich, challenging problem with a wide variety of possible constraints and degrees of freedom available. The solution may differ for each spacecraft mission, with its own operational constraints and desirable mission characteristics.

In the following sections, we study several aspects of the station-keeping problem in order to provide a background for the general problem of station-keeping on a libration orbit. The reader is encouraged to explore different strategies, particularly those surveyed by Folta et al. [231]. We present the results of several analyses, including *tight* and *loose* station-keeping strategies. Typical low-energy lunar transfers are highly constrained, such that there are often not enough degrees of freedom available to the mission designer to employ a loose station-keeping strategy. However, if

the goal of the low-energy lunar transfer is to enter a libration orbit and to remain there, then a loose strategy may be beneficial.

**6.6.2.2 Station-Keeping Simulations** Each of the simulations studied here uses the same set of assumptions, varying only one or two aspects of the station-keeping problem in order to keep the results as comparable as possible. The simulations employ models that are representative of the real solar system, with some simplifications to speed up the computations. The DE421 ephemerides are used to approximate the motion of the Sun, Moon, and planets (Section 2.5.3) and each of the bodies is approximated as a point-mass using the masses presented in Section 2.2. Solar radiation pressure is modeled using a constant solar flux of  $1.019794376 \times 10^{17}$  N and a flat plate model where the mass of the spacecraft is 1000 kg and the surface area is  $10 \text{ m}^2$ . The trajectories are integrated using JPL's Mission-Analysis, Operations, and Navigation Toolkit Environment (MONTE) software (Section 2.7.1).

Each simulation includes a *truth* set of dynamics and an *estimated* set of dynamics, which differ enough to introduce dynamical errors into the navigation problem. The truth set includes the gravitational forces of the Earth, Sun, and Moon and uses a value of 1.00 for the coefficient of radiation of the solar pressure. The estimated set of dynamics also includes the gravitational forces of all of the other planets in the Solar System and uses a value of 1.03 for the coefficient of radiation. These perturbations are somewhat arbitrary and have been selected to approximate the level of accuracy of flight operations.

The reference trajectory for the simulations is a southern halo orbit about the Earth–Moon  $L_2$  point with a  $z$ -axis amplitude of approximately 10,000 km (see Section 2.6.6.3 and Section 2.6.9.4). The reference epoch is January 1, 2017. The perturbations depend on the reference epoch, though they will not likely impact the results very much. It is more likely that the choice of orbit will change the results of the simulations.

Each SKM in each of these simulations is generated using a similar process. First, the state of the spacecraft is propagated from one time to the next using the truth dynamics. At the time of a station-keeping maneuver, the estimated state of the spacecraft at that maneuver is computed by taking the truth state at that time and perturbing it with orbit determination errors. The resulting state is used as the initial state for the station-keeping strategy, whatever it may be. Each station-keeping strategy studied here involves propagating estimated trajectories into the future. These trajectories are propagated using the estimated dynamics, which again differ from the truth dynamics. Once a station-keeping  $\Delta V$  is determined, that  $\Delta V$  is applied to the *true* spacecraft state. Finally, a maneuver execution error is added to the state as well, and the resulting state is propagated using the truth dynamics. This process is repeated for each station-keeping maneuver in the simulation.

The orbit determination errors are modeled as spherically symmetric distributions, such that each of the three Cartesian position coordinates and each of the three Cartesian velocity components is perturbed using independent Gaussian errors, with zero mean and standard deviations of 100 meters (m) for position and 1 millimeter per second (mm/s) for velocity. Hence, the orbit determination errors may be in

any direction, with net  $1\text{-}\sigma$  position uncertainties of approximately 173 m and net  $1\text{-}\sigma$  velocity uncertainties of approximately 1.73 mm/s. These errors are similar in magnitude to those observed by the *ARTEMIS* mission navigators [235]. The maneuver execution error model applies a similar spherically distributed error, such that a Gaussian perturbation of zero mean and 2 mm/s is applied to each of the three components, no matter what size of maneuver it is. Hence, the net  $1\text{-}\sigma$  uncertainty is approximately 3.46 mm/s. The maneuver execution error could be a realization of a burn duration error, an efficiency error, a pressure regulation error, etc. Since it is not clear what is causing the error, the execution error component of the net  $\Delta V$  is not included in any computation of the average or total station-keeping maneuver  $\Delta V$  cost presented below.

Finally, each simulation is repeated at least 30 times to generate statistical results.

**6.6.2.3 Tight Station-Keeping** A very common tight station-keeping strategy is to correct a spacecraft's trajectory in the presence of errors by building each station-keeping maneuver to target the position of the spacecraft's reference trajectory at the time of the following station-keeping maneuver. If all goes well, the station-keeping maneuver will execute perfectly, and the modeled dynamics will perfectly match the true dynamics. In that case, the spacecraft would arrive at the reference trajectory at the time of the next maneuver and perform that maneuver to match its velocity with the reference trajectory. Of course, in reality the spacecraft never arrives precisely on the reference, but must perform another maneuver to correct for additional errors.

Figures 6-19 and 6-20 illustrate this strategy. Figure 6-19 shows a top-down view of the reference halo orbit with a very exaggerated trajectory attempting to follow it. In this case, the SKM are performed at 1-day intervals and the errors are huge, just for visualization purposes. The illustration in Fig. 6-20 shows the difference between the estimated and reference trajectory for a simulation that uses the proper error distributions. The black curve is the truth trajectory, the "x"s indicate the estimated state of the spacecraft at the time of each SKM, and the gray curves illustrate the target trajectories built with the intention to return the spacecraft to the reference.

This tight station-keeping strategy has been applied to a wide range of SKM periods, including periods as short as 0.5 days and as long as 12 days. Figures 6-21 and 6-22 present the resulting range of maneuver  $\Delta V$  costs. One can see many interesting features in the results. First, Fig. 6-21 presents a clear trend such that the average SKM magnitude grows as the duration of time between maneuvers grows. One exception to this is that if the maneuvers are performed too frequently, the average maneuver magnitude rises as the frequent maneuvers fight their collective execution errors. Second, Fig. 6-22 illustrates that there is a minimum in the total expected station-keeping  $\Delta V$  cost that occurs at a period of approximately 3 days, requiring slightly less than 2 m/s per year. If maneuvers are performed more frequently, fuel is wasted combating frequent maneuver execution errors. If maneuvers are performed less frequently, then the spacecraft has more time to drift exponentially away from the reference. Third, the relationships between station-keeping  $\Delta V$  cost and maneuver execution period are very smooth until the maneuvers are executed approximately 7–10 days apart. This duration is slightly longer than half of a revolution period

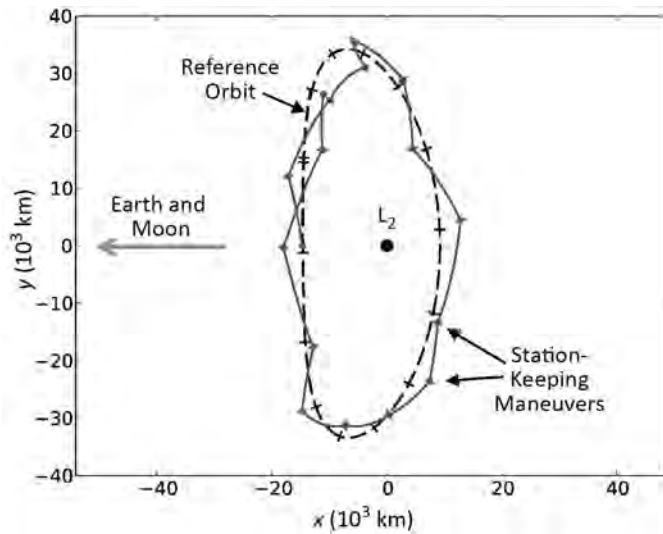


**Figure 6-19** A top-down view of a spacecraft following a reference halo orbit using a tight station-keeping strategy in the presence of very large, exaggerated errors. Station-keeping maneuvers are executed once per day.

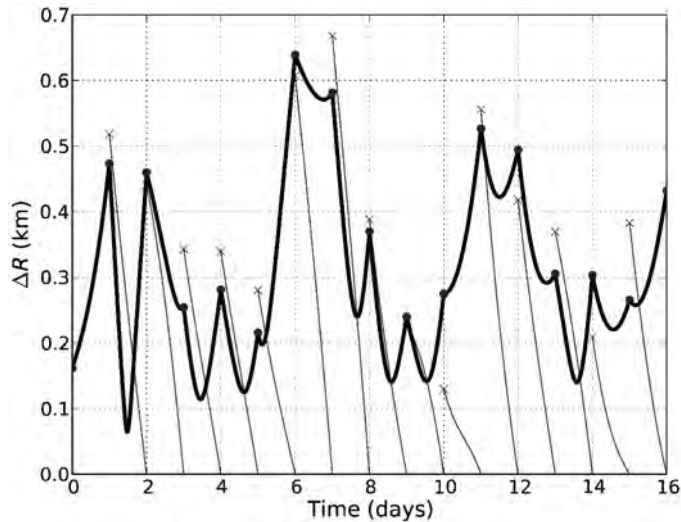


**Figure 6-20** The distance between a spacecraft's trajectory and its reference trajectory for an example tight station-keeping scenario, with maneuvers performed once per day.



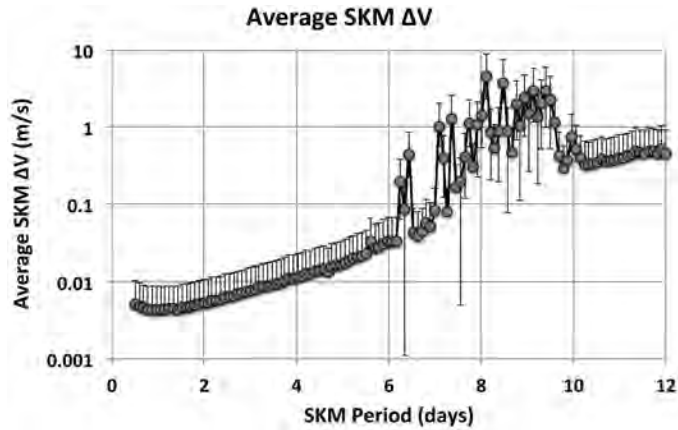


**Figure 6-21** The average station-keeping  $\Delta V$  cost as a function of the duration of time between maneuvers.

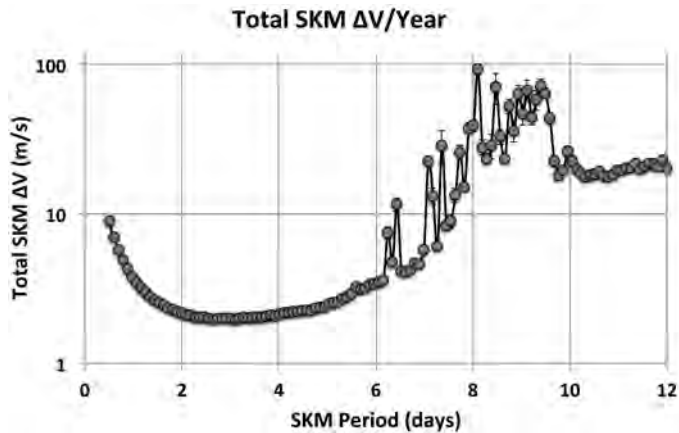


**Figure 6-22** The total annual station-keeping  $\Delta V$  cost as a function of the duration of time between maneuvers.

about the halo orbit. It is hypothesized that the station-keeping sensitivity grows significantly when the target is on the opposite side of the orbit.

Figure 6-22 clearly indicates that if a navigation team intends to reduce the station-keeping cost of a spacecraft on this halo orbit then it is best to perform maneuvers every 2–6 days. From an operational perspective, it is convenient to work on a schedule where a maneuver design cycle is performed every seven days. If the team can support the operational pace, the best strategy may be to design maneuvers every 3.5 days, knowing that if a maneuver is missed then the cost will not grow too high

after 7 days. If this is the case, then it is desirable to estimate the total station-keeping cost of a mission performing approximately two maneuvers per orbit.

The next question is to decide where in the orbit to perform those two maneuvers. Recall from Section 2.6.2.3 that the parameter  $\tau$  may be used to specify a location about a halo orbit, much like the mean anomaly of a conic orbit. We will refer to  $\tau = 0$  deg to be at the  $y = 0$  plane crossing with positive  $y$ -velocity (in the synodic reference frame), and  $\tau$  increases at a constant rate as the spacecraft traverses the orbit. We have simulated scenarios where we have placed one station-keeping maneuver at a  $\tau$  value anywhere from 0 deg to 180 deg and the other station-keeping maneuver at a  $\tau$  value of 180 deg greater than the first. Figures 6-23 and 6-24 illustrate the resulting station-keeping  $\Delta V$  cost of each of these scenarios.

One can draw several conclusions after observing the relationships presented in Figs. 6-23 and 6-24. First, the overall station-keeping cost is roughly the same order of magnitude anywhere around the orbit, except for the spikes observed near  $\tau = 10$  deg and  $\tau = 170$  deg. These spikes are rather unexpected features of these curves. The SKMs become very sensitive to variations at those points in the orbit. In contrast, the best places to perform SKMs on this particular halo orbit are at  $\tau$  values near 30 deg and 150 deg, where the total cost is below 6 m/s per year. Apart from the spikes, the worst locations to perform maneuvers are at  $\tau$  values of 90 deg and 270 deg, namely, where the orbits extend the furthest from the  $y = 0$  plane. It is of interest to note that the station-keeping cost is relatively low at  $\tau$  values of 0 deg and 180 deg, namely, where the orbits cross the  $y = 0$  plane, where they approach the closest and furthest from the Moon, and also where they have their greatest  $z$ -axis excursions.

If the mission operations plan calls for frequent small maneuvers, such that it is okay—and perhaps even expected—to skip a maneuver from time to time, then it is

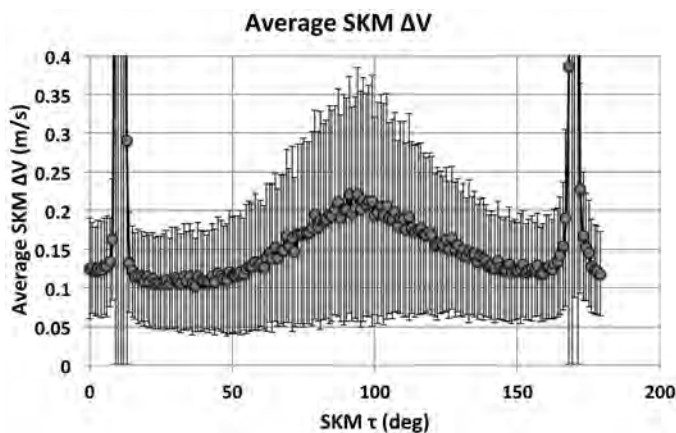


**Figure 6-23** The average station-keeping  $\Delta V$  cost for two maneuvers performed per revolution 180 deg apart in  $\tau$ , as a function of the  $\tau$  value of the first maneuver.

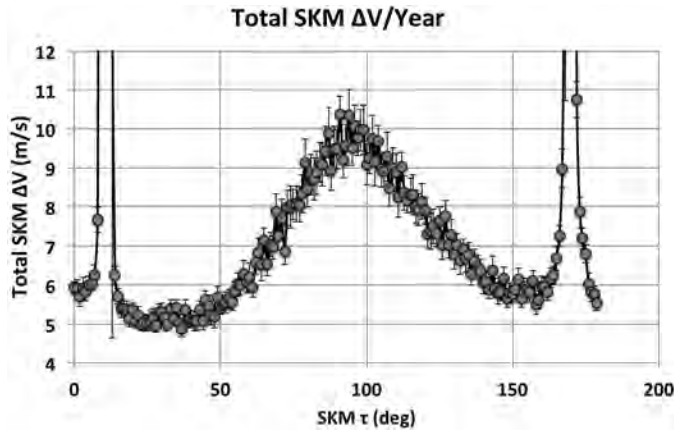


**Figure 6-24** The total annual station-keeping  $\Delta V$  cost for two maneuvers performed per revolution 180 deg apart in  $\tau$ , as a function of the  $\tau$  value of the first maneuver.

of interest to measure the station-keeping cost of a slightly different scenario. In this variation, station-keeping maneuvers are planned every 7 days, but each maneuver is targeted to generate a trajectory that would bring the spacecraft to the reference trajectory in only 3.5 days. In a perfect situation, the trajectory would fly past the reference trajectory halfway between each station-keeping maneuver. In reality it will likely fly past the reference trajectory, though at some distance. Figure 6-25 illustrates the distance between the trajectory and reference of one example instance of this scenario. One can see that the position differences pass very close to zero after most of the maneuvers. Further, the maximum excursions from the reference trajectory rise over time. The figure includes a linear fit and a quadratic fit of the maximum excursions over time, and it is clear that both trends are growing.

This strategy may be generalized in order to understand how the cost of station-keeping depends on the station-keeping period and the duration of time between each SKM and the target state. Numerous simulations are studied here, varying the station-keeping period and the target duration in order to study these relationships. Figure 6-26 illustrates a few example scenarios where the SKMs are performed every day, while their targets are 1, 2, 4, and 5 days into the future. This station-keeping period is likely to be far too rapid for any realistic flight operations, but it is easier to see the features of the plots. One can see that the strategy converges for the cases of 1, 2, and 4, but it does not converge if the target is 5 days into the future. In addition, there is a trend that the spacecraft remains further from the reference trajectory if the SKM targets a point further into the future.

Figures 6-27–6-29 illustrate the results of a wide range of scenarios, where the station-keeping period varies from 1 day to 13 days and the target duration varies from 0.5 days to 24 days. Figure 6-27 presents the total annual station-keeping  $\Delta V$  cost for each combination. Figure 6-28 illustrates the average station-keeping magnitude for

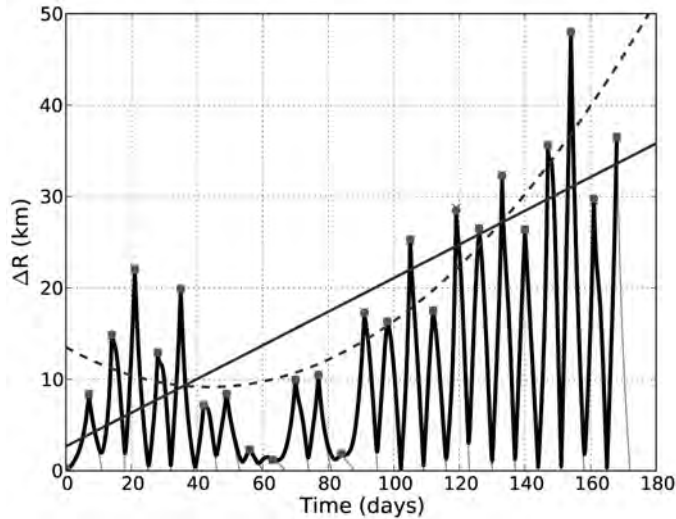


**Figure 6-25** The position difference between the simulated trajectory and the reference trajectory for a scenario where SKMs are performed every 7 days, targeting to the reference trajectory at a point 3.5 days later.

each scenario. Figure 6-29 summarizes the average distance between the resulting trajectory and the reference trajectory for each scenario. In each case, the scenarios shaded white exceed the data range and are not viable station-keeping strategies.

One can draw many conclusions studying these charts. First, if one studies the line of solutions that corresponds to the scenarios where the station-keeping period is equal to the target time, one recovers the results shown in Figs. 6-21 and 6-22. These figures also provide further evidence that the station-keeping performance degrades when the station-keeping period and target time are both around 9 days. It is interesting that there are periodic bands of target durations that converge to successful station-keeping strategies for a given station-keeping period, that is, the three near-vertical dark stripes in each figure. When looking back at Fig. 6-26, it is apparent that some target durations yield scenarios where the trajectories must travel farther from the reference trajectory before returning to the reference. If the station-keeping period is too rapid, or set at an undesirable resonant period, then the distance from the reference trajectory at one SKM is greater than the distance at the previous maneuver, and the strategy diverges.

Nevertheless, the performance of the station-keeping strategy does not significantly improve by targeting a point 10 or more days beyond the given SKM. Statistically there is some benefit derived by permitting the target time to be different than the station-keeping period, though it is typically not far from being equal. Figure 6-30 illustrates this by plotting three curves, tracking the station-keeping performance for 1-, 3-, and 7-day station-keeping periods. One can see that the global minimum of

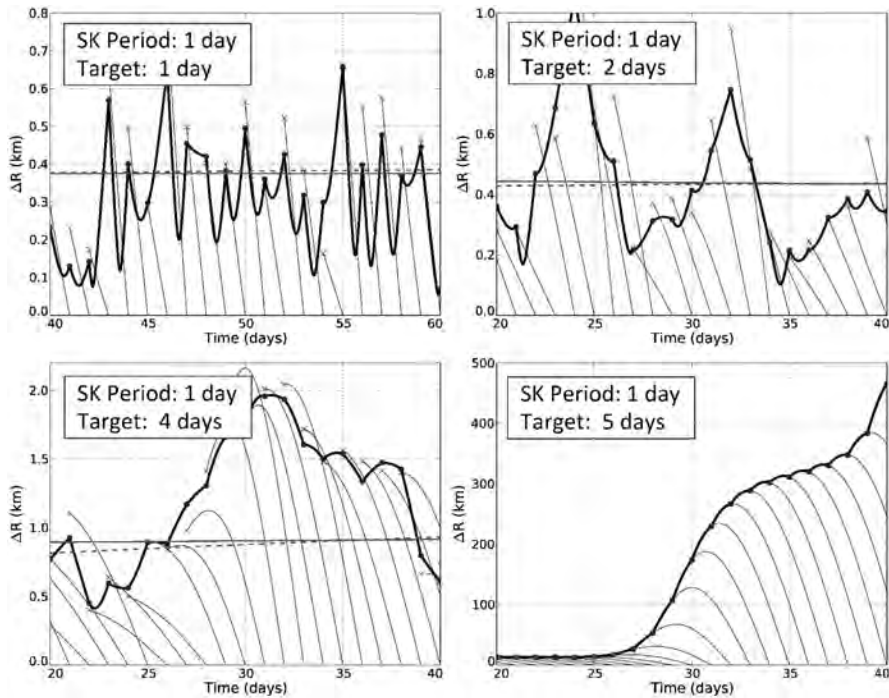


**Figure 6-26** The progression in the position difference between the simulated trajectory and the reference trajectory for scenarios where SKMs are performed every day, but their targets are 1, 2, 4, and 5 days into the future.

each curve shown indeed exists toward the right, where the target duration is around 27 days. But the benefits are slight compared to targeting a few days downstream, which is also a more stable and computationally-efficient station-keeping strategy.

**6.6.2.4 Loose Station-Keeping** A large number of different strategies have been investigated by researchers in order to attempt to reduce the station-keeping  $\Delta V$  cost. We present one such *loose* strategy, namely, a strategy that keeps the spacecraft in the desired region of space without targeting any sort of reference trajectory. For additional strategies, see for example, Folta et al. [231].

The strategy studied here is designed to work for libration orbits and other trajectories that pierce the  $y = 0$  plane with an  $x$ -velocity of approximately zero in the synodic reference frame. Halo orbits pierce the  $y = 0$  plane orthogonally in the circular restricted three-body problem (CRTBP) and nearly orthogonally in a high-fidelity model of the Solar System. Lissajous orbits are permitted to have some nonzero velocity in the  $z$ -axis at those crossings. The loose station-keeping strategy is designed to take advantage of these orbital features.

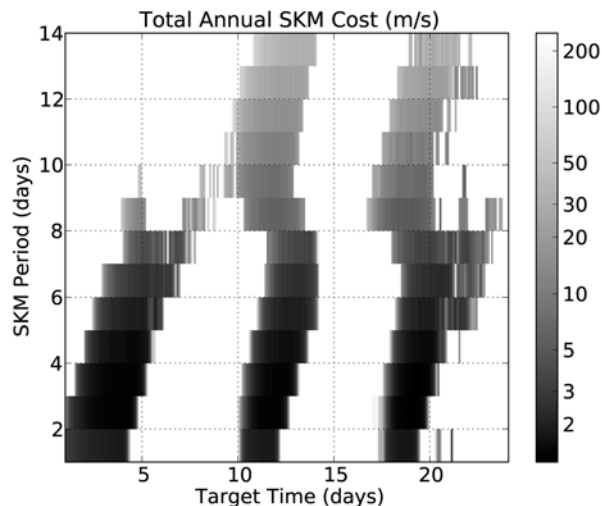


**Figure 6-27** The total annual station-keeping cost for a wide range of scenarios, where the  $x$ -axis sets the amount of time between each SKM and its target point along the reference trajectory, and the  $y$ -axis sets the amount of time between each maneuver and the next.

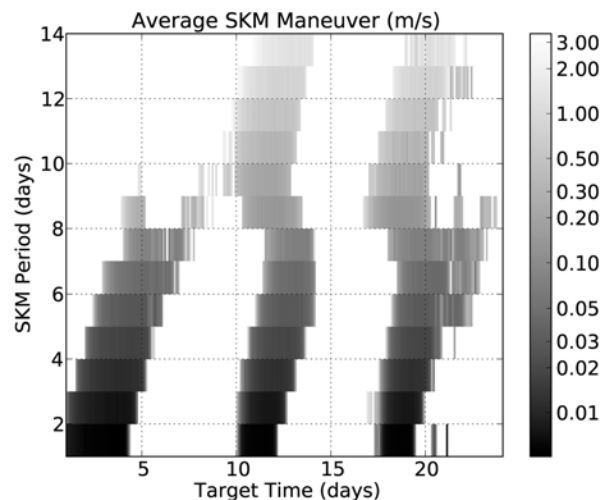


**Figure 6-28** The average SKM magnitude for the same trade space given in Fig. 6-27.

The idea is that a given SKM is designed to target a trajectory that pierces the  $y = 0$  plane orthogonally at either the next crossing or a subsequent crossing. Doing this ensures that the spacecraft remains in the vicinity of its libration orbit for at

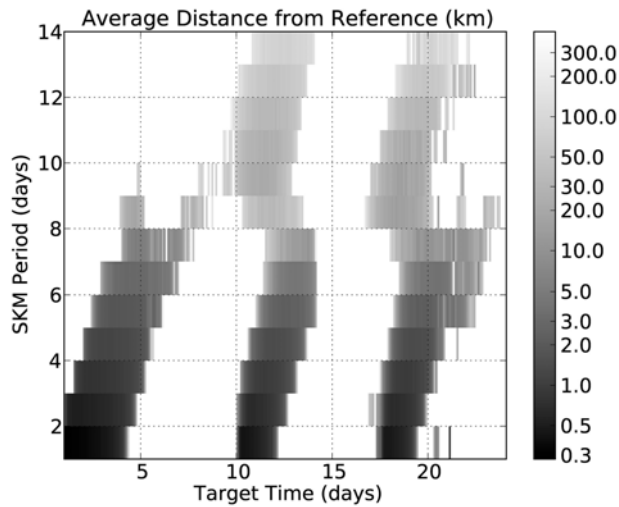


**Figure 6-29** The average distance between the trajectory and the reference trajectory for the same trade space given in Fig. 6-27.

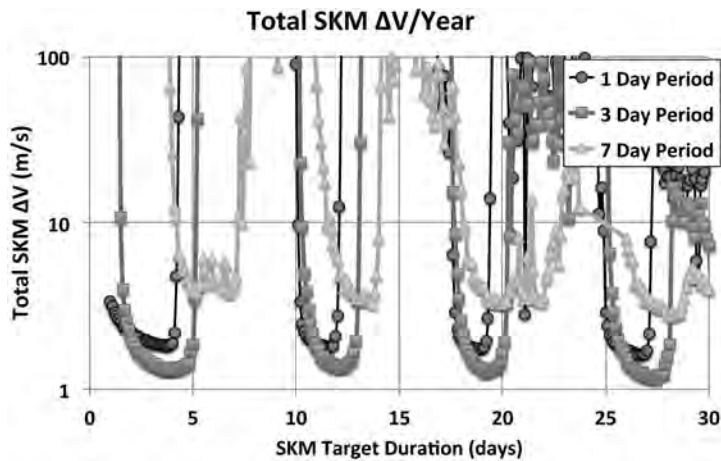


**Figure 6-30** The annual station-keeping  $\Delta V$  cost for three station-keeping periods as functions of the duration between each SKM and the target point along the reference trajectory for that maneuver.

least some time, given the size of the orbit determination and maneuver execution errors. Mission designers typically start the design by targeting the next  $y = 0$  plane crossing to have zero velocity in the  $x$ -axis; once that design is complete it is used to seed a search for a maneuver that pierces the following  $y = 0$  plane crossing with zero velocity in the  $x$ -axis. When targeting the second  $y = 0$  plane crossing, all constraints on the first  $y = 0$  plane crossing are removed. This may be repeated a few times, but modern integrators cannot typically integrate more than two revolutions about a libration orbit (four  $y = 0$  plane crossings) into the future accurately enough to achieve further targets. The further this process extends into the future, the more likely it is that the spacecraft will remain on the particular libration orbit of interest. This algorithm permits the spacecraft's Jacobi constant to change; hence, the spacecraft may wander from one orbit to a neighboring orbit in the state space.

This algorithm has been implemented and tested on scenarios that target the first through fourth  $y = 0$  plane crossing. In each case, each SKM is performed at a  $y = 0$  plane crossing and targets a future  $y = 0$  plane crossing. There may be benefit to placing the SKMs at different  $\tau$  values, or even permitting each maneuver's  $\tau$  value to vary. But these strategies have not been explored here for brevity.

It has been found that a modified single-shooting differential corrector (Section 2.6.5.1 and Section 2.6.6.2) works very well to generate each SKM rapidly. One formulates the problem by permitting the SKM to be in any direction, targeting a state on the subsequent  $y = 0$  plane crossing such that its  $x$ -velocity is zero. The following equation is very similar to Eq. (2.40), modified for this application

$$\begin{bmatrix} \delta x_{T/2} \\ 0 \\ \delta z_{T/2} \\ -\dot{x}_{T/2} \\ \delta \dot{y}_{T/2} \\ \delta \dot{z}_{T/2} \end{bmatrix} \approx \begin{bmatrix} \phi_{11} & \phi_{12} & \phi_{13} & \phi_{14} & \phi_{15} & \phi_{16} \\ \phi_{21} & \phi_{22} & \phi_{23} & \phi_{24} & \phi_{25} & \phi_{26} \\ \phi_{31} & \phi_{32} & \phi_{33} & \phi_{34} & \phi_{35} & \phi_{36} \\ \phi_{41} & \phi_{42} & \phi_{43} & \phi_{44} & \phi_{45} & \phi_{46} \\ \phi_{51} & \phi_{52} & \phi_{53} & \phi_{54} & \phi_{55} & \phi_{56} \\ \phi_{61} & \phi_{62} & \phi_{63} & \phi_{64} & \phi_{65} & \phi_{66} \end{bmatrix} t_{T/2}, t_0 \begin{bmatrix} 0 \\ 0 \\ 0 \\ \delta \dot{x}_0 \\ \delta \dot{y}_0 \\ \delta \dot{z}_0 \\ 0 \end{bmatrix} + \begin{bmatrix} \dot{x} \\ \dot{y} \\ \dot{z} \\ \ddot{x} \\ \ddot{y} \\ \ddot{z} \end{bmatrix} \delta(T/2) \quad (6.1)$$

In this application, the value of  $\delta(T/2)$  may be determined from the second line of Eq. (6.1) to be

$$\delta(T/2) = \frac{-\phi_{24}\delta\dot{x}_0 - \phi_{25}\delta\dot{y}_0 - \phi_{26}\delta\dot{z}_0}{\dot{y}} \quad (6.2)$$

Substituting this value into the fourth line of Eq. (6.1) yields

$$-\dot{x}_{T/2} \approx \phi_{44} - \phi_{24}\frac{\ddot{x}}{\dot{y}} \delta\dot{x}_0 + \phi_{45} - \phi_{25}\frac{\ddot{x}}{\dot{y}} \delta\dot{y}_0 + \phi_{46} - \phi_{26}\frac{\ddot{x}}{\dot{y}} \delta\dot{z}_0 \quad (6.3)$$

One now has a choice about how to construct the SKM. Since there are three degrees of freedom and one control, this algorithm works very well for a mission whose maneuvers are constrained. If there are no further constraints, it is typically



best to build the maneuver that minimizes the  $\Delta V$ . We construct the least squares solution as follows

$$M = \begin{bmatrix} \phi_{44} - \phi_{24} \frac{\ddot{x}}{\ddot{y}}, & \phi_{45} - \phi_{25} \frac{\ddot{x}}{\ddot{y}}, & \phi_{46} - \phi_{26} \frac{\ddot{x}}{\ddot{y}} \end{bmatrix} \quad (6.4)$$

$$\begin{bmatrix} \delta \dot{x}_0 \\ \delta \dot{y}_0 \\ \delta \dot{z}_0 \end{bmatrix} = M^T M M^T{}^{-1} - \dot{x}_{T/2} \quad (6.5)$$

Table 6-5 summarizes the performance of this loose station-keeping strategy for different combinations of maneuver parameters, including the least squares solution  $\overrightarrow{\Delta V}_0$ , and each case where the maneuver is constrained to be in one Cartesian direction (in the Earth–Moon rotating coordinate frame). Further, Table 6-5 includes information for scenarios that target different target  $y = 0$  plane crossings. One can see that the least squares solution performs better than any single-component solution. The  $z$ -axis burns did not converge often enough to characterize their performance for the case when the target was the first  $y = 0$  plane crossing. The table illustrates very clearly that it is significantly better to target the second or third  $y = 0$  plane crossing rather than the first. This makes sense given the amount of oscillation that exists in the system on account of the Moon’s noncircular orbit about the Earth–Moon barycenter. These results suggest that targeting the second  $y = 0$  plane crossing is the most optimal of these loose station-keeping strategies, applied to these particular constraints, errors, and dynamics.

**Table 6-5** A summary of the results of the loose station-keeping strategy explored here.

$y = 0$ Target	$\Delta V$ Type	Avg SKM $\Delta V$ (m/s)		Annual SKM $\Delta V$ (m/s)		Avg Slope from Ref (km/day)
		Mean	1- $\sigma$	Mean	1- $\sigma$	
1	$\overrightarrow{\Delta V}_0$	0.5317	0.3547	25.6863	0.4614	7.9279
1	$\Delta V_0^x$	0.6116	0.4880	29.3714	0.5992	4.3580
1	$\Delta V_0^y$	1.2691	0.7243	61.2268	1.2253	22.4134
1	$\Delta V_0^z$	Failed to converge				
2	$\overrightarrow{\Delta V}_0$	0.0643	0.0525	3.1067	0.1557	1.9986
2	$\Delta V_0^x$	0.0793	0.0613	3.8287	0.1828	1.7720
2	$\Delta V_0^y$	0.1512	0.1455	7.2116	0.3583	2.7830
2	$\Delta V_0^z$	1.2563	1.0133	60.2222	3.7733	12.8971
3	$\overrightarrow{\Delta V}_0$	0.0667	0.0522	3.2276	0.1837	1.9252
3	$\Delta V_0^x$	0.0846	0.0600	4.0560	0.2046	1.4319
3	$\Delta V_0^y$	0.1536	0.1567	7.3782	0.4482	3.2306
3	$\Delta V_0^z$	1.1862	0.9755	56.6230	2.6863	14.4563

If we compare the loose station-keeping strategy studied here with the tight station-keeping strategy considered earlier, we see that the loose strategy performs better for similar station-keeping periods. However, the tight strategy performs better if a mission can perform maneuvers more frequently, on the order of 3–4 days between maneuvers.

**6.6.2.5 Maneuver Execution Errors** All of the results presented previously have kept the spacecraft maneuver execution error model the same, namely, set such that each coordinate of a maneuver's execution is perturbed by an error taken from a normal distribution with mean zero and standard deviation of 2 mm/s. This error model is consistent with the errors observed from the *ARTEMIS* mission. Naturally, the station-keeping  $\Delta V$  budget is dependent on this execution error model. Figure 6-31 presents the annual station-keeping  $\Delta V$  budget as a function of maneuver execution error for a scenario where SKMs are performed at each  $y = 0$  plane crossing, and each maneuver targets the subsequent plane crossing of the reference trajectory. One can see a very linear relationship between the annual  $\Delta V$  cost and maneuver execution error. The line of best fit of this data is equal to

$$\Delta V = 1.8705x + 1.9267 \text{ m/s}$$

The curve's linearity is promising in the sense that the station-keeping strategy has kept the trajectory within the vicinity of the reference trajectory enough that linear approximations are valid. One notices also that the curve does flatten out as the maneuver execution error gets very small. It is in this regime that the orbit determination errors begin to dominate the station-keeping performance.

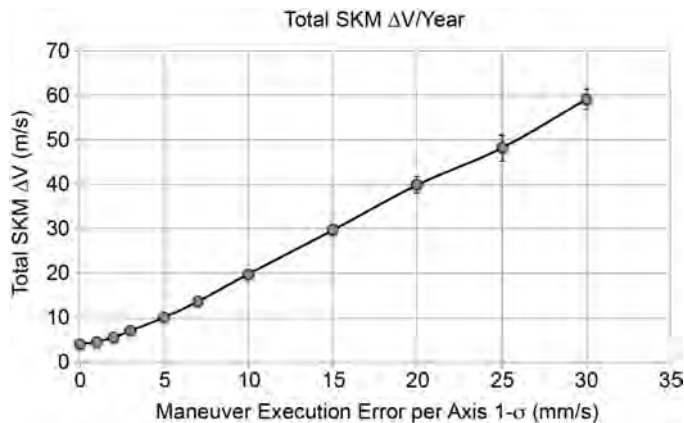


**Figure 6-31** The annual station-keeping  $\Delta V$  cost as a function of maneuver execution errors.

## 6.7 SPACECRAFT SYSTEMS DESIGN

Several considerations must be made to a spacecraft's design when evaluating low-energy lunar transfers compared to conventional lunar transfers. This discussion is meant to guide further analysis and not to reveal a full list of potential issues that one may have with a low-energy transfer, compared with a conventional transfer.

First, low-energy transfers require much more time than conventional transfers between the Earth and the Moon. This impacts the operations schedule, its risk, and its cost. A low-energy transfer's schedule is typically much more relaxed than a conventional transfer's schedule, which must perform a maneuver within a day or even within hours of injection. A spacecraft operations team has much more time to recover from anomalies and safe-mode events when flying a low-energy transfer. The spacecraft team also has more time to characterize the spacecraft, check out the instruments, outgas, and so forth. The mission may even delay maneuvers as needed. In addition, there is much more time to ensure that a spacecraft is on a proper approach vector when arriving at the Moon via a low-energy transfer than a conventional transfer.

The communications systems for spacecraft traversing low-energy transfers must be capable of reaching out to 1–2 million kilometers, depending on the transfer. This is 3–5 times further than a conventional transfer. This long link distance may require larger ground station antennas, larger spacecraft antennas, and/or more communications power. However, a spacecraft intending to perform its mission objectives at the Moon may not have much data to transmit at its apogee passage, alleviating some of the pressures caused by the long link distance.

A low-energy transfer requires a smaller maneuver when arriving at the Moon, compared with a conventional transfer to the same destination. This fact may benefit a lunar mission in many ways. First, the spacecraft does not require as much fuel and can put more of the  $\Delta V$  requirements on the launch vehicle rather than the spacecraft. Second, the spacecraft may reduce the amount of gravity losses when performing an insertion into a low lunar orbit using small engines. This was the case for the two *GRAIL* spacecraft, and it could be the case for any lunar landers. Finally, a mission to a lunar libration orbit does not even require a large orbit insertion maneuver, which may open up many design options.

Low-energy transfers commonly traverse through regions of space where the Sun–Earth–spacecraft angle and/or the Sun–spacecraft–Earth angle drops near zero degrees. This characteristic may be detrimental to the communications system on board the spacecraft, though it may only impact the mission for a day or two.

The final consideration presented here is that low-energy transfers typically do not pass through the Van Allen Belts more than once, which may reduce the radiation risks for a lunar spacecraft, compared with a conventional transfer that may implement Earth-phasing orbits.

